Dressing of Proton with Virtual Pions in a Nuclear Model with Explicit Mesons

Dressing af Proton med Virtuelle Pioner i en Kernemodel med Eksplicitte Pioner

Martin Cradock Østerlund
201804897

Master's Thesis in Physics
June 2023

Supervisor: Dmitri Fedorov

Department of Physics and Astronomy
Aarhus University

Colophon

Dressing of Proton with Virtual Pions in a Nuclear Model with Explicit Mesons

— Dressing af Proton med Virtuelle Pioner i en Kernemodel med Eksplicitte Pioner

Master's thesis by Martin Cradock Østerlund. Written under supervision by Dmitri Fedorov, Department of Physics and Astronomy, Aarhus University.

Typeset by the author with LaTeX and the memoir document class, using Linux Libertine and Linux Biolinum 11.0/13.6pt.

The various scripts I have made for numerical simulations, along with figures generated for this thesis are available at https://github.com/MCOsterlund/Master-Thesis

Printed at Aarhus University

Abstract (English)

The purpose of this thesis is to investigate the dressing of a nucleon with two virtual pions in the nuclear model with explicit mesons. In this model the nucleons interact with mesons explicitly, on the same level as the nucleons, rather than through phenomelogical potentials. We will be considering the dressing of protons with just pions, and we will consider the case where the nucleon is dressed by two pions.

We introduce the method of correlated Gaussians, where the wavefunction of a quantum mechanical system can be written as a linear combination of correlated Gaussians. Solving the Schrödinger equation for such a system ammounts to solving a generalized eigenvalue problem, that must be optimized with respect to linear and non-linear parameters, in order to find the ground state energy of the given system. We then introduce the nuclear model with explicit mesons in greater detail, and consider the special case of a nucleon dressed by two explicit pions. In this model, different systems of nucleons dressed with increasing number of mesons are coupled together with a creation operator, which has only two parameters: A coupling strength and a range parameter. We derive the shape of the wavefunctions needed to describe the system, along with the matrix elements needed to solve the generalized eigenvalue problem. For this purpose we develop a general expansion method for calculating the matrix elements using correlated Gaussians, which involves Taylor expanding the analytical shape of the matrix elements of shifted Gaussians to the given order needed.

We then perform numerical simulations on the effect of the dressing of the second pion. We begin by solving the dressing of a nucleon with a single pion. This serves as a proof of conept for the method, and also shows how many Gaussians are needed in our linear combination to accurately describe the system. We then introduce the dressing of the second pion, and compare its contribution to the total system with the contribution from the first pion at different values of the coupling parameters. We show that the coupling strength has a negligible effect on the contribution of the second pion, but increasing the range parameter drastically increases the influence of the second pion, to the point where a one-pion approximation is no longer sufficient for a fully accurate description.

Resumé (Dansk)

Formålet med dette speciale er at undersøge koblingen mellem en nukleon og to pioner i en kernemodel med eksplicitte mesoner. I denne model interagerer mesonerne ikke igennem fænomenologiske potentialer men optræder eksplicit på samme niveau som nukleonerne selv. Vi vil i dette speciale udelukkende fokuserer på koblingen mellem nukleoner og pioner, og vi begrænser os til en kobling med to eksplicitte pioner.

Vi benytter os af en metode, hvor bølgefunktionen af et kvantemekanisk system kan opskrives som en linear kombination af korrelerede Gauss funktioner. Løsningen til Schrödinger ligningen kan i så fald omskrives til et generaliseret egenværdi problem, som skal optimeres mht. lineære og ikke lineære parametre, for at finde systemets grundtilstands energi. Dernæst introduceres kernemodellen med eksplicitte mesoner i større detalje, og vi betragter særtilfældet hvor kernen er koblet til to pioner. I denne model kobles systemer med et stigende antal mesoner sammen igennem en operator, som kun har to parametre: En koblingsstyrke og en koblingsafstand. Vi udleder de nødvendige bølgefunktioner for at beskrive systemet, samt matrix elementerne der skal bruges til at løse det generaliserede egenværdi problem. Til det formål udvikles en generel udvidelses metode, som involverer en rækkeudvikling af den analytiske form af matrix elementerne af skiftede Gauss funktioner til den påkrævede orden.

Dernæst udføres en række numeriske simuleringer, hvor effekten af koblingen med den anden pion er blevet undersøgt. Først løses systemet hvor nukleonen er koblet til en enkelt pion. Denne løsning fungerer som en illustration af modellen og undersøger samtidig antallet af Gauss funktioner der skal benyttes i vores linearkombination af bølgefunktionen for at få en præcis beskrivelse. Dernæst introduceres koblingen med den anden pion, og bidraget til det totale system sammenlignes med bidraget fra den første pion ved forskellige værdier af koblingsparametrene. Vi viser at koblingsstyrken har negligibel effekt på koblingen af den anden pion, men at en stigning i koblingsafstanden øger bidraget fra den anden pion drastisk, endda til et punkt hvor at den anden pion skal medtages for at få en fuldt nøjagtig beskrivelse.

Preface

This thesis concludes my Master's degree at the Department of Physics and Astronomy at Aarhus University under the supervision of Dmitri Fedorov. The purpose of this thesis was to expand upon the nuclear model with explicit mesons, in order to account for the dressing of a second pion in the model. I would like to thank my supervisor Dmitri Fedorov for supervising my project, and for the discussions we have had about the subject throughout the process. I have learned a great deal about numerical methods and new theory.

I would also like to think my office colleagues Camilla Theresia Grøn Sørensen, Christiane Rahbek, Erik Steenberg, Hans Brüner Dein and Jacob Bay Thomsen for the good company we have enjoyed throughout this year. A special thanks to Jacob for revising the thesis.

Lastly, I would like to thank my friends and family for their support and companionship through the year.

Contents

Chapter 1

Introduction

With the discovery of the neutron in 1932, it became clear that atomic nuclei consisted of protons and neutrons bound together. But with the neutron having neutral charge, the binding to the positive proton could not be explained using Coulomb interaction. Therefore, a new concept was created to accomodate this new discovery: The strong nuclear interaction [1]. The next question was how this strong interaction could be described.

An attempt was made in 1935 by Hideki Yukawa, who proposed that the nucleons would exchange particles between eachother, similarly to how the mediator for the electromagnetic force is the photon, which is a massless particle. In this case however, the particles would have a mass the fraction of the Nucleons themselves.[2] These mediating particles would eventually be called mesons, and are essential for describing the strong nuclear interaction between nucleons and the binding of nuclei [1]. There are many known mesons, but of special interest in this thesis are the isoscalar pions $\left(\pi^0, \pi^-, \pi^+\right)$, which have a mass of around $140MeV$. These are the lightest of the mesons, with the nucleons being roughly 7 times as heavy as the pions. Given the pions' long Compton wavelength of around $1.4fm$, the pion is responsible for the long range interaction of the nuclear force [3].

Since Yukawa's initial theory, many attempts at making a theory describing the interaction between nucleons and mesons have been made: From early field theories, to simple one-boson exchange theories, to the more modern and refined chiral effective field theories [1, 4, 5]. Common for all of these is the introduction of some phenomenological potential, which adequately describes the nucleon-nucleon interaction. The mesons, while being a part of these theories, are treated implicitly in favor of these potentials.

1.1 A Nuclear Model With Explicit Mesons

In this thesis, we consider a different approach, where the mesons are treated explicitly on the same footing as the nucleons themselves. Previous works have worked as a proof of concept for this method. A nuclear model with an explicit scalar σ-mesons

have been shown to yield reasonable binding energies for the bound state of the deuteron [6]. Similarly, a more advanced model with a single explicit pion has given good results in the description of neutral pion photoproduction off protons [7]. In this thesis, we take a step further in the development of this model, discussing the dressing of a nucleon with two explicit pions.

1.2 Outline of Thesis

The purpose of this thesis is to construct the nuclear model with explicit pions in the two-pion approximation, and then document the effect of the second pion on the dressing of the nucleon. In chapter 2, we describe the relevant theory needed to construct the model and perform numerical calculations. We begin by introducing the method of Shifted Correlated Gaussians, where the wavefunction of a quantum mechanical system is expanded in a linear combination of shifted Gaussians. We then show how we can use the matrix elements of shifted Gaussians to find the corresponding matrix elements of unshifted Gaussians, which will be the main tool used in this thesis. Then, we show how we can find the energy of a system by solving a generalized eigenvalue problem. For this purpose, we need the matrix elements between Gaussians, and we will see that these can be found analytically. At the end of chapter 2, we briefly discuss different algorithms that can be used to solve the aforementioned generalized eigenvalue problem to find the ground state energy. In chapter 3, we introduce the nuclear model with explicit mesons, with a special focus on explicit pions. We begin by introducing a general system of a nucleon dressed by a number of pions, which serves as a primer for the introduction of the one and two-pion approximation. In chapter 3 we also introduce the relative Jacobi coordinate transform, which can be used to reduce the dimensionality of the system, and decrease the computational load. Lastly, we go in depth with the one and two pion systems, deriving the wavefunctions that satisfy the correct boundary conditions. In chapter 4, we use the explicit form of the wavefunctions found in chapter 3 to derive the matrix elements used to calculate the dressing of a nucleon. We begin by deriving a general form of the matrix elements, which can, in practice, be used for a multitude of few-body systems. Using this general method, we derive the explicit shape of the matrix elements used for numerical calculations of both the one-pion and the two-pion system. We also introduce another proposed method for finding matrix elements, that wasn't used in this thesis due to complications with the kinetic matrix elements. In chapter 5, we compare the contribution to the total wavefunction of the one-pion and the two-pion systems. We show the difference in dressing energy between the two systems, and discuss the effect of the second pion.

Chapter 2

Theoretical background

In this chapter, we explain the relevant theory necessary for solving the system of a nucleon coupled to two pions. This method is frequently used when solving few body systems numerically [8]. First, we introduce the concept of Gaussian basis functions and shifted Correlated Gaussians. We show how, by expanding the wavefunction into a linear combination of Gaussians, the Schrödinger equation can be written as a generalized eigenvalue problem with analytical matrix elements. Then we discuss different methods that can be used to solve this generalized eigenvalue problem numerically. We will primarily consider the stochastic variational method and compare it to a more direct optimization, where local minimizers are used for solving the system.

2.1 Shifted Correlated Gaussians

In this section, we will describe the use of explicitly correlated Gaussians in calculating matrix elements for various systems. The method of correlated Gaussians sees use in treatments of small nucleons, but also simple atoms can be treated using this expansion [9].

Considering an arbitrary wavefunction, $|\psi\rangle$, we can write this as a linear combination of Gaussians [10],

$$|\psi\rangle = \sum_{i=1}^{n_g} c_i |g_i\rangle, \tag{2.1}$$

where n_g is the number of Gaussians used in the expansion, and where the Gaussians can be written in coordinate space as

$$\langle \mathbf{r}|g\rangle = exp\left(-\sum_{i,j}^{n_g} A_{ij}\vec{r}_i \cdot \vec{r}_j + \sum_{i=1}^{n_g} \vec{s}_i \cdot \vec{r}_i \right) = e^{-\mathbf{r}^T A\mathbf{r}+\mathbf{s}^T\mathbf{r}} \tag{2.2}$$

In eq. (2.2), $\mathbf{r}$ is a size n_g column vector of spacial coordinate vectors

$$\mathbf{r} = \begin{pmatrix} \vec{r}_1 \\ \vec{r}_2 \\ \vdots \\ \vec{r}_N \end{pmatrix}, \tag{2.3}$$

A is an $n_g \times n_g$ matrix of parameters, and $\mathbf{s}$ is a size n_g column vector of shift vectors. These simply shift the location of the Gaussians, which are normally centered around the origin, a given distance away from the origin. For the purposes of this thesis, the matrix A will be parameterized according to the following equation:

$$A = \sum_{i<j}^{n_g} \frac{w_{ij} w_{ij}^T}{b_{ij}^2} \tag{2.4}$$

where w_{ij} is a vector of size n_g where the $i'th$ element is 1 and the $j'th$ element is -1, and b_{ij} is some parameter that is characteristic to the range of interaction that we consider. In this thesis, b_{ij} is drawn from an exponential distribution,

$$b_{ij} = -ln(u)b \tag{2.5}$$

where u is a quasi random number drawn from a Halton sequence, such that $u \in]0, 1[$ while b is a characteristic range for the system [11].

Notice that by inserting eq. (2.4) into eq. (2.2), we get the sum,

$$\begin{aligned} -\mathbf{r}^T A \mathbf{r} &= -\mathbf{r}^T \sum_{i<j}^{n_g} \frac{w_{ij} w_{ij}^T}{b_{ij}^2} \mathbf{r} = -\mathbf{r}^T \sum_{i<j}^{n_g} \frac{w_{ij} w_{ij}^T}{b_{ij}^2} \mathbf{r} = -\sum_{i<j}^{n_g} \frac{(\mathbf{r}^T w_{ij})(w_{ij}^T \mathbf{r})}{b_{ij}^2} \\ &= -\sum_{i<j}^{n_g} \frac{\left(\vec{r}_i - \vec{r}_j\right)^2}{b_{ij}^2} \end{aligned} \tag{2.6}$$

so an interpretation of w_{ij} is the vector that picks out the relative coordinates between two particles. Similarly to w_{ij}, we will also be using the vector w_i, which has a 1 in entry i and zeros everywhere else, such that $\vec{r}_i = w_i^T \mathbf{r}$.

The terms in equation 2.2 are known as Shifted Gaussians, and this choice of basis is especially useful in cases where the coordinates of the nuclei are considered to be fixed. One should note however that if the coordinates of the nuclei are not fixed, then the shifted gaussians are not eigenfunctions of the square of the total angular momentum, unless the shift is zero. [8]

The method of shifted correlated Gaussians has the benefit of yielding analytic matrix elements when working with multi-body systems, which makes it much easier to calculate energies and states for such systems [10]. Applying the wavefunction in equation 2.1 to the Schrödinger equation,

$$\hat{H}|\psi\rangle = E|\psi\rangle \tag{2.7}$$

and then multiplying by $\langle\psi|$ from the right, we can find the energy of the system by using the variational method [12].

$$E = \frac{\sum_{k,k'}^{N} c_k c_{k'} \langle A_k|\hat{H}|A_{k'}\rangle}{\sum_{k,k'}^{N} c_k c_{k'} \langle A_k|A_{k'}\rangle} = \frac{c^T \mathcal{H} c}{c^T \mathcal{N} c} \tag{2.8}$$

where c is a size-N vector of eigenvectors, $\mathcal{H}$ is an $N \times N$ symmetric matrix with matrix elements $\langle A_k|\hat{H}|A_{k'}\rangle$, and $\mathcal{N}$ is an $N \times N$ symmetric positive definite matrix with matrix elements $\langle A_k|A_{k'}\rangle$. We want to find the values of c that minimizes the energy. Taking the derivative of eq. (2.8) with respect to one of the eigenvectors, c_k, we can write, noting that the overlap between Gaussians is nonzero.

$$\frac{\partial E}{\partial c_k} = 2\frac{(Hc)_k \left(c^T \mathcal{N} c\right) - \left(c^T \mathcal{H} c\right)(Nc)_k}{\left(c^T \mathcal{N} c\right)^2} \tag{2.9}$$

where $(Hc)_k$ and $(Hc)_k$ indicates a sum over all the terms in $c^T \mathcal{H} c$ and $c^T \mathcal{N} c$ that contains c_k. Then, we can use eq. (2.8) to write $\left(c^T \mathcal{H} c\right) = E\left(c^T \mathcal{N} c\right)$. Inserting this in eq. (2.9) and setting the derivative equal to zero.

$$\frac{\partial E}{\partial c_k} = 2\frac{(Hc)_k - E\,(Nc)_k}{\left(c^T \mathcal{N} c\right)} = 0 \rightarrow (Hc)_k - E\,(Nc)_k = 0 \tag{2.10}$$

Doing this for all of the eigenvectors, we get the following generalized eigenvalue problem.

$$\mathcal{H} c = E \mathcal{N} c \tag{2.11}$$

Equations eq. (2.11) is the key equation when finding the optimal parameters for our system. There are two parameters that need to be optimized in order to find the minimal energies: The eigenvectors, c, and the optimal values for the non-linear parameters, A and A' in eq. (2.8). The methods used to find these quantities will be described in the next section.

The matrix elements needed to solve eq. (2.11) is the overlap between two Gaussians, the overlap of the Gaussians with the Hamiltonian and the overlap with a Coulomb form factor, $\frac{1}{w_{ij}^T \mathbf{r}}$. The general form of the matrix elements when using shifted Gaussians have been found and derived in [10]. A more in-depth derivation of the matrix elements can be found in appendix A. The general form of these matrix elements are as follows:

Overlap:

$$\langle e^{-\mathbf{r}A\mathbf{r}+s'^T\mathbf{r}}|e^{-\mathbf{r}B\mathbf{r}+s^T\mathbf{r}}\rangle = e^{\frac{1}{4}(s+s')^T R(s+s')}\left(\frac{\pi^{n_g}}{det(C)}\right)^{3/2} \equiv M \tag{2.12}$$

where n_g indicates the number of Gaussians and $C = A + B$.

Kinetic Energy:

$$\begin{aligned}&\langle e^{-\mathbf{r}A\mathbf{r}+s'^T\mathbf{r}}|\hat{K}|e^{-\mathbf{r}B\mathbf{r}+s^T\mathbf{r}}\rangle \\ &= \Big(6Trace(AKBR) + \big(s' - AR(s+s')\big)^T K \big(s - BR(s+s')\big)\Big) M\end{aligned} \tag{2.13}$$

where $\hat{K} = -\frac{\partial}{\partial \mathbf{r}} K \frac{\partial}{\partial \mathbf{r}^T}$, and K is symmetric positive definite matrix.

Coulomb Potential:

$$\langle G'|\frac{1}{|w^T\mathbf{r}|}|G\rangle = M\frac{erf\left(\sqrt{\beta}q\right)}{q} \tag{2.14}$$

where $\beta = (w^T R w)^{-1}$, $q = \frac{1}{2}w^T R(s+s')$ and erf is the error function. In principle, one can use these shifted Gaussians to calculate numerical systems. However, they are in general not eigenfunctions of the total angular momentum [8]. To circumvent this, we will be using standard non-shifted Gaussians.

$$|g\rangle = e^{-\mathbf{r}^T A\mathbf{r}} \tag{2.15}$$

These unshifted Gaussians can be shown to be eigenfunctions of the total angular momentum. More specifically, eq. (2.15) can be shown to be an eigenfunction of the total angular momentum with eigenvalue 0. For this reason, we dub them the S-wave expansion, similar to atomic orbitals with orbital quantum number $l = 0$. From these unshifted Gaussians, equations with higher order angular momentum, such as P- and D-waves with $l = 1$ and $l = 2$ respectively. We refer to chapter 4 for a derivation of these higher order matrix elements, and we refer to appendix B for an explicit example, where the Hydrogen wavefunctions have been written using Gaussians with higher order angular momentum.

The unshifted Gaussians in eq. (2.15) are simply the shifted Gaussians from eq. (2.2), but with the shiftvectors set to zero. This means that the matrix elements of unshifted Gaussians are similar to that of shifted Gaussians, only with the shiftvectors set to zero. The matrix elements for unshifted Gaussians are therefore [6, 10]:

Overlap:

$$\langle e^{-\mathbf{r}A\mathbf{r}}|e^{-\mathbf{r}B\mathbf{r}}\rangle = \left(\frac{\pi^N}{det(C)}\right)^{3/2} \equiv M_0 \tag{2.16}$$

Kinetic Energy:

$$\langle e^{-\mathbf{r}^T A\mathbf{r}}|\hat{K}|e^{-\mathbf{r}^T B\mathbf{r}}\rangle = 6Trace(AKBR)M_0 \tag{2.17}$$

Coulomb term

$$\frac{erf\left(\sqrt{\beta}q\right)}{q}M \xrightarrow{q\to 0} \frac{2}{\sqrt{\pi}}\sqrt{\beta}M_0 \tag{2.18}$$

2.2 Methods for solving the generalized eigenvalue problem

We need to solve the generalized eigenvalue problem, eq. (2.11), for the linear parameters, c and the non-linear parameters A, as described in section 2.1. Solving for the linear parameters is straightforward, and involves just a method for solving a standard generalized eigenvalue problem. Since the matrix $\mathcal{N}$ is positive definite, we can find an invertible matrix, Q such that $Q^T\mathcal{N}Q$ and $Q^T\mathcal{H}Q$ are both diagonal and real. Additionally, since $\mathcal{N}$ and $\mathcal{H}$ in eq. (2.11) and since $\mathcal{N}$ is positive definite by construction, the energy eigenvalues in eq. (2.11) are real [13]. So a general method to diagonalize matrices can be applied to solve the system and the solution is guarenteed to yield real eigenvalues and eigenvectors. For this thesis, we shall simply use the eigh module from scipy, which uses LAPACK drivers to solve the symmetric eigenvalue problem [14, 15]

Finding the non-linear parameters, A and A' requires more advanced algorithms. One approach is to use the Stochastic Variational Method. In this method, we generate random guesses for the parameters, and check whether the elements give a lower energy. Assume we have a basis of $k-1$ elements, that gives an energy E_{k-1}. The step for finding a lower energy then goes as follows:

1. Generate a number, N, of basis elements, $A_1^k, A_2^k, \ldots A_N^k$ via random sampling.
2. Solve the eigenvalue problem, eq. (2.11), by adding each of the N basis elements to the size $k-1$ basis individually. This generates N new energies, $E_1^K, E_2^k \ldots E_N^k$.
3. Let's assume the parameter A_i^k produced the energy E_i^k, which is the lowest. The parameter A_i^k is then added to the basis, making it a size k basis. Repeat until convergent.

This is a rather fast algorithm, since it doesn't require the Hamiltonian to be recalculated at every iteration, nor does it require a full rediagonalization every time a new basis element is selected [16].

The method used in this thesis uses a more direct approach. In this method we generate a size-n_g basis of random or quasi random numbers (for example via a Halton sequence.) We then use the Nelder-Mead Downhill Simplex method to find the minimal energy [17]. This is a bit more intensive since we are varying all N basis elements at the same time. As such, this method runs extremely slow if N is very large. Additionally, one should note that the Nelder-Mead algorithm is a local minimizer. That means that there is a risk that the algorithm might terminate at a local minima instead of the desired global minima. This can be offset by running the algorithm several times with different starting parameters, for example using random sampling, and cross referencing the results.

Unless otherwise specified, it can be assumed that the Downhill Simplex method is used throughout the remainder of this thesis. The amount of basis elements used rarely exceeds 10, which means the Downhill Simplex method still runs sufficiently fast. Additionally, it is easy to implement using Python libraries such as SciPy [15].

Chapter 3

A Nuclear Model With Explicit Pions

In this chapter, we explain the nuclear model with explicit pions. The nucleus of an atom is held together by the strong nuclear force, which is mediated by mesons. One of the primary mediators of the strong force is the pion, which is responsible for the long-range interactions of the strong force due to its Compton wavelength of around $1.4fm$ [3]. While the nuclear interaction between nucleons and mesons is typically considered through the construction of phenomenological potentials or quantum field theories, in this thesis we treat pions on the same foot as the nucleons, as explicit particles [1, 18].

3.1 The Nuclear Model with Explicit Pions

It is well established that a so-called bare nucleon is dressed by a cloud of pions to create what we know as the physical nucleon or, more appropriately for this thesis, the dressed nucleon [19]. Pions can only be emitted by the nucleon and become a physical pion, if they exceed a potential barrier of about $140MeV$, which is roughly the mass of the pion. If less than this amount of energy is applied, the pion remains under the potential barrier and is considered a virtual pion. An illustration of this can be seen in fig. 3.1. A dressed nucleon can then be seen as a superposition of a "bare" nucleon, which isn't dressed by pions, and several different states dressed with a different number of pions. This is described by the wavefunction in eq. (3.1).

$$\Psi = \begin{pmatrix} \psi_{\tilde{N}} \\ \psi_{\tilde{N}\pi} \\ \psi_{\tilde{N}\pi\pi} \\ \vdots \end{pmatrix}, \tag{3.1}$$

where $\psi_{\tilde{N}}$ is the wavefunction of the bare nucleon, and the other terms represent the nucleon being dressed by an increasing number of pions as indicated by the subscript. The Hamiltonian that acts on this multi componenent wavefunction is as follows:

$$H = \begin{pmatrix} K_{\tilde{N}} + \check{m}_{\tilde{N}} & W^{\dagger} & 0 & \dots \\ W & K_{\tilde{N}} + \check{m}_{\tilde{N}} + K_{\pi_1} + \check{m}_{\pi_1} + V_C & W^{\dagger} & \dots \\ 0 & W & K_{\tilde{N}} + \check{m}_{\tilde{N}} + K_{\pi_1} + K_{\pi_2} + \check{m}_{\pi_1} + \check{m}_{\pi_2} + V_C & \dots \\ \vdots & \vdots & \vdots & \ddots \end{pmatrix} \tag{3.2}$$

Where $K_{\tilde{N}}$ is the kinetic term for the bare nucleon,

$$K_{\tilde{N}} = \frac{-\hbar^2}{2m_{\tilde{N}}} \frac{\partial^2}{\partial \vec{r}^2_{\tilde{N}}}, \tag{3.3}$$

with $\vec{r}_{\tilde{N}}$ being the coordinate to the nucleon, K_π are the kinetic terms for the pions,

$$K_{\pi_i} = \frac{-\hbar^2}{2m_{\pi_i}} \frac{\partial^2}{\partial \vec{r}^2_i}, \tag{3.4}$$

with $\vec{r}_i$ being the coordinates for the pions, $\check{m}_{\tilde{N}} = m_{\tilde{N}}c^2$ and $\check{m}_{\pi_i} = m_{\pi_i}c^2$ with $m_{\tilde{N}}$ and m_{π_i} being the mass of the bare nucleon and the mass of the i'th pion respectively. The terms, V_C are included to account for potential Coulomb interactions.[7]

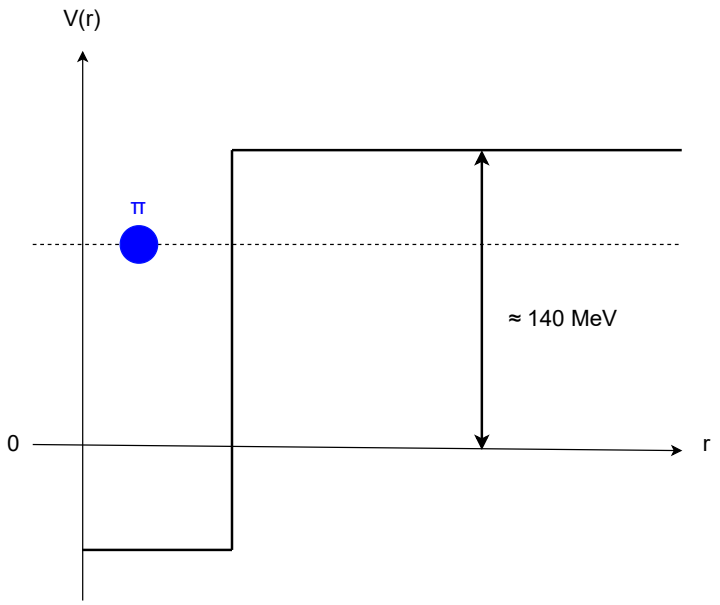

FIGURE 3.1: An illustration of a single virtual pion. The pion dresses the nucleon and is under a potential of about $140MeV$, roughly equal to the physical mass of the pion[20].

The different subsystems are coupled together by an operator, W, which couples the systems of different pions together. Since nuclear interactions must conserve total

angular momentum, isospin and parity, the operator coupling the different systems must do the same. The pion is an isospin triplet, that has spin zero and negative intrinsic parity. In order to account for this, we introduce the coupling constants:

$$W = (\bar{\tau}\bar{\pi})(\bar{\sigma}\bar{r})f(r) \tag{3.5}$$

$$W^{\dagger} = \int d^3\bar{r}(\bar{\tau}\bar{\pi})(\bar{\sigma}\bar{r})f(r) \tag{3.6}$$

where

$$\bar{\tau}\bar{\pi} = \tau_0\pi^0 + \sqrt{2}\tau_-\pi^+0 + \sqrt{2}\tau_+\pi^- \tag{3.7}$$

with $\bar{\tau}$ being the isospin matrices of the nucleons.

$$\tau_0 = \begin{pmatrix} 1 & 0 \\ 0 & -1 \end{pmatrix}, \quad \tau_- = \begin{pmatrix} 0 & 0 \\ 1 & 0 \end{pmatrix}, \quad \tau_+ = \begin{pmatrix} 0 & 1 \\ 0 & 0 \end{pmatrix} \tag{3.8}$$

$\bar{\pi}$ is the three states of the pion, $\bar{\sigma}$ are the three pauli spin matrices, and $\bar{r}$ are the spatial coordinates [18, 21]. Note the added integral in equation 3.6, which removes the coordinate of the annihilated pion. The function, $f(r)$ is a short-ranged form factor, which controls the range of the interaction between the created pion and the nucleon. In principle we are free to choose the form factor as we please, but in order to properly emulate the finite ranges of the nuclear forces, they must be decreasing functions of the distance between the particles, r. Throughout this thesis we will use a Gaussian form factor:

$$f(r) = \frac{S_W}{b_W} e^{-\frac{r^2}{b_W^2}} \tag{3.9}$$

where b_W is a range parameter controlling the range of the interaction, and S_W is the coupling strength between the nucleon and the pion. The negative exponent in eq. (3.9) ensures the coupling goes to zero with increasing r, and since the product of two Gaussians is a Gaussian, it is well suited when using the method of correlated Gaussians.

It is worth quickly noting that some literature cites a pion creation operator, W in eq. (3.5), with a gradient over the spatial coordinates, as is the case in [18].

$$W_{alt} = (\vec{\tau}\cdot\vec{\pi})(\vec{\sigma}\cdot\nabla_{\vec{r}})f(r) \tag{3.10}$$

However, carrying out the derivative in eq. (3.10) on our Gaussian form factor in eq. (3.9) reveals that the expressions in eq. (3.10) and eq. (3.5) are equivalent up to a common factor.

3.2 Notation and the Jacobi Coordinate Transform

Before we begin discussing the specific cases of the one pion and two pion dressing, we first discuss the use of the Jacobi coordinate transform. Up until now, we have considered the spherical coordinates of individual particles. Instead, we can use the transformation to relative Jacobi coordinates, which is described by the following equations:

$$\vec{x}_j = \frac{\sum_{k=1}^{j} m_k \vec{r}_k}{\sum_{k=1}^{j} m_k} - \vec{r}_{j-1}, \quad j = \{1, \dots N-1\} \tag{3.11}$$

$$\vec{R} = \frac{\sum_{k=1}^{M} m_k \vec{r}_k}{\sum_{k=1}^{M} m_k} \tag{3.12}$$

where $\vec{x}_j$ are the relative coordinates between two particles, while $\vec{R}$ is the center of mass coordinate. A visual demonstration of the change of coordinates can be see in fig. 3.2.

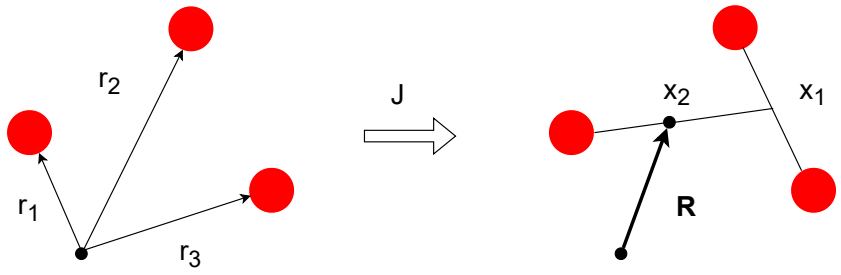

FIGURE 3.2: The same system of three particles in two different sets of coordinates. On the left are regular spherical coordinate, while on the right, the system is expressed in relative Jacobi coordinates.

For a general N-particle system, the Jacobi coordinate transformation can also be written as a matrix.

$$J = \begin{pmatrix} 1 & -1 & 0 & 0 & \dots & 0 \\ \frac{m_1}{M2} & \frac{m_2}{M2} & -1 & 0 & \dots & 0 \\ \vdots & \vdots & \vdots & \vdots & \ddots & \vdots \\ \frac{m_1}{M_{N-1}} & \frac{m_2}{M_{N-1}} & \dots & \dots & \dots & -1 \\ \frac{m_1}{M_N} & \frac{m_2}{M_N} & \dots & \dots & \dots & \frac{m_{\tilde{N}}}{m_{\tilde{N}}} \end{pmatrix} \tag{3.13}$$

where

$$M_i = \sum_{k=1}^{i} m_k \tag{3.14}$$

such that the full transformation can be written in a convenient shorthand form

$$\mathbf{x} = J\mathbf{r} \tag{3.15}$$

where

$$\mathbf{x} = \begin{pmatrix} \vec{x}_1 \\ \vec{x}_2 \\ \vdots \\ \vec{R} \end{pmatrix} \tag{3.16}$$

which is similar to how we defined the vector **r** in section 2.1. It can be shown that the Jacobian matrix in eq. (3.13) has determinant 1, which means that the mathematical shape of the matrix elements are preserved under a coordinate transform. This is true as long as we also remember to transform the kinetic matrix K from eq. (2.17) and the vectors w_{ij}. These transform according to

$$K \to JKJ^T \tag{3.17}$$

$$w_{ij} \to U^T w_{ij}, \tag{3.18}$$

where $U = J^{-1}$ [6].

The advantage of the relative Jacobi coordinates is that we can discard the center of mass coordinate, $\vec{R}$, as long as there are no external forces acting on the system. This is equivalent to removing the last row of the matrix J and the last column of U. This means that the transformed K and w_{ij} from eq. (3.17) and eq. (3.18) have dimensions $n_g - 1 \times n_g - 1$ and $n_g - 1$ respectively. The dimensionality of the system as a whole is reduced by 1, which lowers the computational load of the system significantly [6, 16].

3.3 Dressing of the Nucleon in the One Pion System

We are now ready to discuss how the nucleons are dressed by pions, and the shape of the wavefunctions that describe each system. Since the two-pion description of the nucleon requires a coupling between the one-pion system and the two-pion system, we begin by treating just the one-pion system. The wavefunction that describes this system is

$$\Psi_1 = \begin{pmatrix} \psi_{\tilde{N}} \\ \psi_{\tilde{N}\pi} \end{pmatrix} \tag{3.19}$$

with $\psi_{\tilde{N}}$ being the wavefunction of the bare nucleon, while $\psi_{\tilde{N}\pi}$ is the wavefuntion for the bare nucleon dressed by one pion. The wavefunction is normalized under the condition that the total wavefunction Ψ_1 is normalized to unity.

$$\int_V |\Psi_1|^2 dV = \int_V \left(|\psi_{\tilde{N}}|^2 + |\psi_{\tilde{N}\pi}|^2 \right) dV = 1 \tag{3.20}$$

where dV indicates and integral over all the spatial coordinates in the system. The untransformed Hamiltonian of the one-pion system is a simpler version of the general matrix Hamiltoninan from eq. (3.2) and can be seen in eq. (3.21).

$$H = \begin{pmatrix} \hat{K}_{\tilde{N}} + \check{m}_{\tilde{N}} & W^{\dagger} \\ W & \hat{K}_{\tilde{N}} + \check{m}_{\tilde{N}} + \hat{K}_{\tilde{N}\pi} + \check{m}_{\pi} \end{pmatrix} \tag{3.21}$$

The kinetic operator for the nucleon is

$$\hat{K}_{\tilde{N}} = -\frac{\hbar^2}{2m_{\tilde{N}}} \frac{\partial^2}{\partial \vec{r}_N} \tag{3.22}$$

and for the pion-Nucleon system we have

$$\hat{K}_{\tilde{N}\pi} = K_{\tilde{N}} + K_{\pi_1} = -\frac{\partial}{\partial \mathbf{r}_{\tilde{\mathbf{N}}\pi}} K_{\tilde{N}\pi} \frac{\partial}{\partial \mathbf{r}_{\tilde{\mathbf{N}}\pi}{}^T} \tag{3.23}$$

where the derivatives are column vectors of the form

$$\frac{\partial}{\partial \mathbf{r}_{\tilde{\mathbf{N}}\pi}} = \begin{pmatrix} \frac{\partial}{\partial \vec{r}_{\tilde{N}}} \\ \frac{\partial}{\partial \vec{r}_{\pi}} \end{pmatrix} \tag{3.24}$$

and $K_{\tilde{N}\pi}$ is a 2×2 diagonal matrix

$$K_{\tilde{N}\pi} = \begin{pmatrix} \frac{\hbar^2}{2m_{\tilde{N}}} & 0 \\ 0 & \frac{\hbar^2}{2m_{\pi}} \end{pmatrix} \tag{3.25}$$

We now perform the transform to the relative Jacobi coordinates. This is especially simple for the bare nucleon system, since it just involves moving to the rest frame of the bare proton. This also means that the kinetic operator for the bare nucleon, eq. (3.22) vanishes, which suggests that the wavefunction for the bare nucleon system is a constant. We choose the following form:

$$\psi_{\tilde{N}} = \frac{p \uparrow}{\sqrt{V}} \tag{3.26}$$

where p is the isospin state of the nucleon corresponding to a proton

$$p = \begin{pmatrix} 1 \\ 0 \end{pmatrix} \tag{3.27}$$

and $\uparrow$ corresponds to the system being in a spin up state

$$\uparrow = \begin{pmatrix} 1 \\ 0 \end{pmatrix} \tag{3.28}$$

The system is normalized so as to contain one proton in the volume, V. Had the system been chosen as a neutron with another spin orientation, the subsequent treatment would have been similar.

Notice that we have removed the Coulomb terms in eq. (3.21). We can apply the operator $\left(\vec{\tau} \cdot \vec{\pi}\right)$ from eq. (3.7) to the state of the proton to see that it is in a coherent superposition

$$\left(\vec{\tau} \cdot \vec{\pi}\right) p = p\pi^0 + \sqrt{2} n \pi^+ \tag{3.29}$$

where n is the state of the neutron. Given that π^0 and n are electrically neutral, there are no Coulomb interactions when considering this system. This changes later when we consider the two pion system. In this case however, the Coulomb terms can be seen as a small correction compared to the nuclear forces, and can therefore be neglected. We refer to appendix appendix D for a demonstration of why omitting the Coulomb interactions is a small correction.

Performing the Jacobi transform of the one-pion part of the system, the kinetic operator $K_{\tilde{N}\pi}$ becomes

$$\hat{K}_{\tilde{N}\pi} \to \frac{-\hbar^2}{2m_{\tilde{N}\pi}} \frac{\partial^2}{\partial \vec{r}} \tag{3.30}$$

where $\vec{r}$ is the relative coordinate between the pion and the nucleon, and $m_{N\pi}$ is the reduced mass of the system

$$m_{\tilde{N}\pi} = \frac{m_{\tilde{N}} m_\pi}{m_{\tilde{N}} + m_\pi} \tag{3.31}$$

The full transformed Hamiltonian matrix can then be written as

$$H = \begin{pmatrix} \check{m}_{\tilde{N}} & W^\dagger \\ W & \hat{K}_{\tilde{N}\pi} + \check{m}_{\tilde{N}} + \check{m}_\pi \end{pmatrix} \tag{3.32}$$

Using the matrix in eq. (3.32), we can write out the Schrödinger equation of the system. In matrix form, rewriting $\tilde{E} = E - \check{m}_{\tilde{N}}$, this becomes

$$H\Psi = \tilde{E}\Psi \to \begin{pmatrix} 0 & W^\dagger \\ W & \hat{K}_{\tilde{N}\pi} + \check{m}_\pi \end{pmatrix} \begin{pmatrix} \psi_{\tilde{N}} \\ \psi_{\tilde{N}\pi} \end{pmatrix} = \tilde{E} \begin{pmatrix} \psi_{\tilde{N}} \\ \psi_{\tilde{N}\pi} \end{pmatrix} \tag{3.33}$$

Writing out the matrix eq. (3.33) and using the explicit shape of the operators W and $W^\dagger$

$$\int_V d^3r \left(\vec{\tau}\cdot\vec{\pi}\right)^\dagger \left(\vec{\sigma}\cdot\vec{r}\right)^\dagger \psi_{\tilde{N}\pi} = \tilde{E}\psi_{\tilde{N}} \tag{3.34}$$

$$\left(\vec{\tau}\cdot\vec{\pi}\right)\left(\vec{\sigma}\cdot\vec{r}\right)\psi_{\tilde{N}} + (\hat{K}_{\tilde{N}\pi} + \check{m}_\pi)\psi_{\tilde{N}\pi} = \tilde{E}\psi_{\tilde{N}\pi} \tag{3.35}$$

We note that, because of eq. (3.35), the wavefunction $\psi_{\tilde{N}\pi}$ must have the same spin-isospin structure as the creation operator in eq. (3.5). This suggests the following form of the wavefunction, $\psi_{\tilde{N}\pi}$.

$$\psi_{\tilde{N}\pi}(r) = \left(\vec{\tau}\cdot\vec{\pi}\right)\left(\vec{\sigma}\cdot\vec{r}\right)\frac{p\uparrow}{\sqrt{V}}\phi(r) \tag{3.36}$$

where $\phi(r)$ is a scalar function. The function must have dimensions $[length]^{-5/2}$ in order to make the integral

$$\int_V d^3R \int_V d^3r |\psi_{\tilde{N}\pi}|^2 \tag{3.37}$$

dimensionless. Additionally, if we assume the form-factor, $f(r)$ is finite and short ranged, then $\phi(r)$ must also satisfy the boundary conditions

$$\begin{aligned} \phi(0) &= const \\ \phi(\infty) &= 0 \end{aligned} \tag{3.38}$$

A candidate solution that satisfies the boundary conditions in eq. (3.38) and the dimensionality constraint in eq. (3.37) are the one-dimensional Gaussians of the form.

$$\phi(r) = \sum_{i=1}^{n_g} c_i e^{-\alpha_i r^2} \tag{3.39}$$

where c_i are the eigenvectors found by solving eq. (2.11) and α_i is a one-dimensional parameter that is parameterized similarly to eq. (2.4) [7].

3.4 Dressing of the Nucleon in the Two Pion System

We are now ready to discuss the dressing of the bare nucleon with a second pion. The wavefunction for the full system then becomes

$$\Psi_2 = \begin{pmatrix} \psi_{\tilde{N}} \\ \psi_{\tilde{N}\pi} \\ \psi_{\tilde{N}\pi\pi} \end{pmatrix} \tag{3.40}$$

where $\psi_{\tilde{N}}$ and $\psi_{\tilde{N}\pi}$ are the bare and one pion contributions to the wave function, and where $\psi_{\tilde{N}\pi\pi}$ is the wavefunction for the bare nucleon being dressed by two pions. As with eq. (3.19), Ψ_2 is normalized to unity.

$$\int_V |\Psi_2|^2 dV = \int_V |\psi_{\tilde{N}}|^2 + |\psi_{\tilde{N}\pi}|^2 + |\psi_{\tilde{N}\pi\pi}|^2 dV = 1 \tag{3.41}$$

where dV again indicates an integration over all the spatial coordinates of the system. The full two-pion Hamiltonian in the untransformed coordinates can be written as (where we have gotten rid of the Coulomb terms preemptively)

$$H = \begin{pmatrix} K_{\tilde{N}} + \check{m}_{\tilde{N}} & W^\dagger & 0 \\ W & K_{\tilde{N}} + \check{m}_{\tilde{N}} + K_{\pi_1} + \check{m}_{\pi_1} & W^\dagger \\ 0 & W & K_{\tilde{N}} + \check{m}_{\tilde{N}} + K_{\pi_1} + K_{\pi_2} + \check{m}_{\pi_1} + \check{m}_{\pi_2} \end{pmatrix} \tag{3.42}$$

where W_1 creates the first pion for the system, while W_2 creates the second pion. The treatment of the bare nucleon and the one-pion system has been done in section 3.3 and for Ψ_2, the treatment of these systems is similar. As such, we just need to treat the two-pion component of eq. (3.42). The kinetic operator in the two-pion system reads as

$$\hat{K}_{N\pi\pi} = K_{\tilde{N}} + K_{\pi_1} + K_{\pi_2} = -\frac{\partial}{\partial \mathbf{r}_{\mathrm{N}\pi\pi}} K_{N\pi\pi} \frac{\partial}{\partial \mathbf{r}_{\mathrm{N}\pi\pi}{}^T} \tag{3.43}$$

with

$$\frac{\partial}{\partial \mathbf{r}_{\mathrm{N}\pi\pi}} = \begin{pmatrix} \frac{\partial}{\partial \vec{r}_{\pi_1}} \\ \frac{\partial}{\partial \vec{r}_{\pi_2}} \\ \frac{\partial}{\partial \vec{r}_N} \end{pmatrix}, \quad K_{N\pi\pi} = \begin{pmatrix} \frac{\hbar^2}{2m_{\pi_1}} & 0 & 0 \\ 0 & \frac{\hbar^2}{2m_{\pi_2}} & 0 \\ 0 & 0 & \frac{\hbar^2}{2m_{\tilde{N}}} \end{pmatrix} \tag{3.44}$$

Performing the Jacobi coordinate transform on the two-pion system, we can choose the relative coordinates in three different ways, see figs. 3.3 to 3.5 [9].

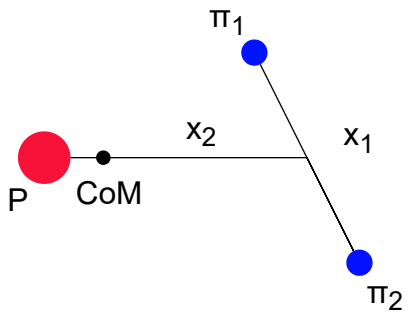

FIGURE 3.3: Relative Jacobi coordinates where the first relative coordinate is between the two pions.

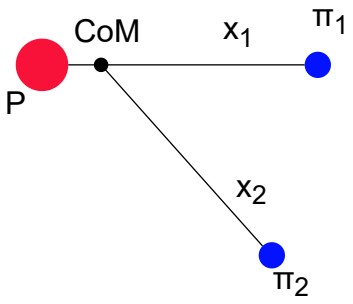

FIGURE 3.4: Relative Jacobi coordinates where the first relative coordinate is between the nucleon and the first pion.

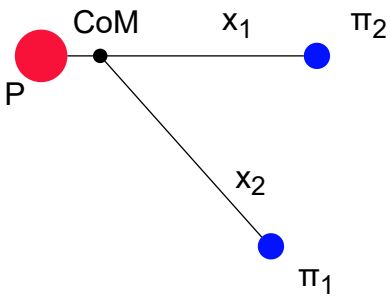

FIGURE 3.5: Relative Jacobi coordinates where the first relative coordinate is between the nucleon and the second pion.

All three coordinate transforms in figs. 3.3 to 3.5 give the same result, so choosing a coordinate set is a matter of convenience and personal choice. We will generally be

using the form in fig. 3.3, since we can assume the pion masses to be identical, and so many of the terms simplify. Naming the relative coordinate between the pions $\vec{x}_1$ and the relative coordinates between nucleon and the two pions $\vec{x}_2$, the Jacobi transformed kinetic matrix in eq. (3.44) becomes.

$$K_{N\pi\pi} = \begin{pmatrix} \frac{\hbar^2}{2m_{\pi\pi}} & 0 \\ 0 & \frac{\hbar^2}{2m_{N\pi\pi}} \end{pmatrix} \tag{3.45}$$

with the reduced masses

$$m_{\pi\pi} = \frac{m_\pi^2}{2m_\pi} = \frac{1}{2}m_\pi, \quad m_{N\pi\pi} = \frac{2m_\pi m_{\tilde{N}}}{2m_\pi + m_{\tilde{N}}} \tag{3.46}$$

Then, similarly to how it was done in eq. (3.21), we can generate the matrix Hamiltonian.

$$H\Psi = \tilde{E}\Psi \rightarrow \begin{pmatrix} 0 & W_1^\dagger & 0 \\ W_1 & \hat{K}_{\tilde{N}\pi} + \check{m}_{\pi_1} & W_2^\dagger \\ 0 & W_2 & \hat{K}_{\tilde{N}\pi\pi} + 2\check{m}_\pi \end{pmatrix} \begin{pmatrix} \psi_{\tilde{N}} \\ \psi_{\tilde{N}\pi}(\vec{r}) \\ \psi_{\tilde{N}\pi\pi}(\vec{x}_1, \vec{x}_2) \end{pmatrix} = \tilde{E} \begin{pmatrix} \psi_{\tilde{N}} \\ \psi_{\tilde{N}\pi}(\vec{r}) \\ \psi_{\tilde{N}\pi\pi}(\vec{x}_1, \vec{x}_2) \end{pmatrix} \tag{3.47}$$

Writing out eq. (3.47) in a set of coupled equations, we get

$$\int_V d^3r \left(\vec{\tau}\cdot\vec{\pi}\right)^\dagger \left(\vec{\sigma}\cdot\vec{r}\right)^\dagger \psi_{\tilde{N}\pi} = \tilde{E}\psi_{\tilde{N}} \tag{3.48}$$

$$\left(\vec{\tau}\cdot\vec{\pi}_2\right)\left(\vec{\sigma}\cdot\vec{r}\right)\psi_{\tilde{N}} + (\hat{K}_{N\pi} + \check{m}_\pi)\psi_{N\pi} + \int d^3x_2 \left(\vec{\tau}\cdot\vec{\pi}\right)^\dagger \left(\vec{\sigma}\cdot\vec{x}_2\right)^\dagger f(x_2)\psi_{\tilde{N}\pi\pi} = \tilde{E}\psi_{\tilde{N}\pi} \tag{3.49}$$

$$\left(\vec{\tau}\cdot\vec{\pi}_2\right)\left(\vec{\sigma}\cdot\vec{x}_2\right) f(x_2)\psi_{\tilde{N}\pi} + (\hat{K}_{N\pi\pi} + 2\check{m}_\pi)\psi_{\tilde{N}\pi\pi} = \tilde{E}\psi_{\tilde{N}\pi\pi} \tag{3.50}$$

Same as for the one-pion case, we can write $\psi_{\tilde{N}\pi}$ as a function of a scalar function, $\phi(r)$, that satisfies the boundary conditions in eq. (3.38). This can solved by using the same Gaussian expansion as in eq. (3.39). However, the parameters α and c_i are not generally expected to have the same value as in the one-pion system, due to the additional coupling with the two-pion system. Given that the spin-isospin structure must be preserved between systems, eq. (3.50) suggests the following shape of the $\psi_{\tilde{N}\pi\pi}$ wavefunction:

$$\psi_{\tilde{N}\pi\pi}(x_1, x_2) = \left(\vec{\tau}\cdot\vec{\pi}_2\right)\left(\vec{\sigma}\cdot\vec{x}_2\right)\left(\vec{\tau}\cdot\vec{\pi}_1\right)\left(\vec{\sigma}\cdot\vec{x}_1\right)\frac{p\uparrow}{\sqrt{V}}\rho(x_1, x_2) \tag{3.51}$$

which now adds another boundary condition on top of the ones we found in section 3.3

$$\begin{aligned} &\rho(0,0) = const. \\ &\rho(\infty, x_2) = 0 \\ &\rho(x_1, \infty) = 0 \end{aligned} \tag{3.52}$$

The equation solving ρ can again be chosen as a Gaussian expansion, this time of the form

$$\rho(x_1, x_2) = \sum_{i=1}^{n_g} c_i e^{-\mathbf{x}^T A \mathbf{x}} \tag{3.53}$$

where $\mathbf{x}$ is a size two vector containing the coordinates $\vec{x}_1$ and $\vec{x}_2$, and where A is a 2×2 matrix parameterized according to eq. (2.4).

3.5 Setting up the Generalized Eigenvalue Matrices

With the shape of the wavefunctions in place, we can now set up the matrices $\mathcal{H}$ and $\mathcal{N}$ to solve the generalized eigenvalue problem in eq. (2.11). The matrix $\mathcal{H}$ is simply the overlap of the relevant wavefunctions with each of the elements in the Hamiltonian matrix eq. (3.47).

$$\mathcal{H} = \begin{pmatrix} 0 & \langle\psi_{\tilde{N}}|W_1^\dagger|\psi_{\tilde{N}\pi}\rangle & 0 \\ \langle\psi_{\tilde{N}\pi}|W_1|\psi_{\tilde{N}}\rangle & \langle\psi_{\tilde{N}\pi}|\hat{K}_{\tilde{N}\pi}|\psi_{\tilde{N}\pi}\rangle + \check{m}_{\pi_1}\langle\psi_{\tilde{N}\pi}|\psi_{\tilde{N}\pi}\rangle & \langle\psi_{\tilde{N}\pi}|W_2^\dagger|\psi_{\tilde{N}\pi\pi}\rangle \\ 0 & \langle\psi_{\tilde{N}\pi}|W_2|\psi_{\tilde{N}\pi\pi}\rangle & \langle\psi_{\tilde{N}\pi\pi}|\hat{K}_{\tilde{N}\pi\pi}|\psi_{\tilde{N}\pi\pi}\rangle + 2\check{m}_\pi\langle\psi_{\tilde{N}\pi\pi}|\psi_{\tilde{N}\pi\pi}\rangle \end{pmatrix} \tag{3.54}$$

Each of the diagonal elements in eq. (3.54) are block matrices. The blocks are square matrices of size n_{g_1} and n_{g_2}, with n_{g_1} and n_{g_2} being the amount of Gaussians used to expand the one pion system and the two pion system respectively. Since the first term in the diagonal doesn't use any Gaussians, it is simply one dimensional. The overlaps with the raising and lowering operator terms are similarly on a block form, such as to fit in with the square block matrices along the diagonal. Similarly, we can use that the overlap between different pion systems is zero to construct the matrix $\mathcal{N}$.

$$\mathcal{N} = \begin{pmatrix} 1 & 0 & 0 \\ 0 & \langle\psi_{\tilde{N}\pi}|\psi_{\tilde{N}\pi}\rangle & 0 \\ 0 & 0 & \langle\psi_{\tilde{N}\pi\pi pi}|\psi_{\tilde{N}\pi\pi}\rangle \end{pmatrix} \tag{3.55}$$

As such, all we need to solve the generalized eigenvalue problem is to find the matrix elements in eq. (3.54) and eq. (3.55) under the constraints imposed by ϕ and ρ, and the mass of the bare proton chosen such that when we add the energy to the mass of the bare nucleon, we get the physical mass of the physical nucleon.

$$m_N = m_{\tilde{N}} + \tilde{E} \tag{3.56}$$

So in practice, for each Gaussian added we must first solve the system with the condition $\check{m}_{\tilde{N}} = \check{m}_N$ in order to find an an intermediate energy, $\tilde{E}_0$, and then solve the system again with $m_{\tilde{N}} = m_N - \tilde{E}_0$, repeating the process until the change in $\check{m}_{\tilde{N}}$ is satisfactory [7].

The matrix elements of eq. (3.54) and eq. (3.55) are found in chapter 4

Chapter 4

Matrix Elements of Pion Subsystems

In this chapter, we derive the matrix elements that are used in eq. (3.54) and eq. (3.55) above. We begin by deriving a general method to calculate matrix elements, that will be applied to both the one pion and the two pion system. Then, we will apply this general method to the two systems, by writing out the the spin-space part of the wavefunction. Lastly, we discuss some alternative methods to calculate the matrix elements that were considered, but ultimately didn't see use.

4.1 A General Expansion of the Matrix Elements

The matrix elements we presented in section 2.1 are insufficient for calculating the matrix elements in section 3.5, since we see that the overlap of wavefunctions eq. (3.19) and eq. (3.40) will include the relative coordinates of the pions. As such, we must derive further matrix elements to account for these coordinates. In order to demonstrate the method, we will be using the overlap, but this method is applicable to the overlap with operators in general. This method closely follows a similar method presented in [10] for the treatment of tensor potentials.

So far we have only expanded the matrix elements we found in section 2.1 to the lowest possible order, our so called S-wave expansion. We will look to write the wavefunctions of our pions systems in a higher order expansion, which we adequately will call the P- and D-wave expansion, since these states will have orbital angular momentum quantum numbers $l = 1$ and $l = 2$ respectively. For some coordinate set, $\mathbf{r}$, they are

$$g^{(P)} = \left(\mathbf{a}^T\mathbf{r}\right) e^{-\mathbf{r}^T A\mathbf{r}} \tag{4.1}$$

$$g^{(D)} = \left(\mathbf{a}^T\mathbf{r}\right)\left(\mathbf{b}^T\mathbf{r}\right) e^{-\mathbf{r}^T A\mathbf{r}} \tag{4.2}$$

where $\mathbf{a}$ and $\mathbf{b}$ are parameter vectors of size-n_g. Their specific form is system dependent, and will be discussed in section 4.2 and section 4.3. Taking the overlap with our new expansions, the overlaps become

$$\langle g'^{(P)}|g^{(P)}\rangle = \langle e^{-\mathbf{r}^T A\mathbf{r}} \left(\mathbf{a}^T\mathbf{r}\right) | \left(\mathbf{b}^T\mathbf{r}\right) e^{-\mathbf{r}^T B\mathbf{r}}\rangle \tag{4.3}$$

$$\langle g'^{(D)}|g^{(D)}\rangle = \langle e^{-\mathbf{r}^T A\mathbf{r}} \left(\mathbf{a}^T\mathbf{r}\right)\left(\mathbf{b}^T\mathbf{r}\right) | \left(\mathbf{c}^T\mathbf{r}\right)\left(\mathbf{d}^T\mathbf{r}\right) |e^{-\mathbf{r}^T B\mathbf{r}}\rangle \tag{4.4}$$

The overlaps in eq. (4.3) and eq. (4.4) are the matrix elements of which we want to find an analytical form. To do this we, we rewrite the two equations to use shifted Gaussians instead of unshifted Gaussians.

$$\langle G'^{(P)}|G^{(P)}\rangle = \langle e^{-\mathbf{r}^T A\mathbf{r}+s'^T\mathbf{r}} \left(\mathbf{a}^T\mathbf{r}\right) | \left(\mathbf{b}^T\mathbf{r}\right) e^{-\mathbf{r}^T B\mathbf{r}+s^T\mathbf{r}}\rangle \tag{4.5}$$

$$\langle G'^{(D)}|G^{(D)}\rangle = \langle e^{-\mathbf{r}^T A\mathbf{r}+s'^T\mathbf{r}} \left(\mathbf{a}^T\mathbf{r}\right)\left(\mathbf{b}^T\mathbf{r}\right) | \left(\mathbf{c}^T\mathbf{r}\right)\left(\mathbf{d}^T\mathbf{r}\right) |e^{-\mathbf{r}^T B\mathbf{r}+s^T\mathbf{r}}\rangle \tag{4.6}$$

While we don't know the value of the overlap with these parameters, notice now that we can take the derivatives with respect to s, s' of eq. (4.5) and eq. (4.6) in order to rewrite the equations into a form where we can express them in terms of the overlap of shifted Gaussians. This allows us to rewrite the overlaps.

$$\langle G'^{(P)}|G^{(P)}\rangle = \left(\mathbf{a}^T\frac{\partial}{\partial s'^T}\right)\left(\mathbf{b}^T\frac{\partial}{\partial s^T}\right)\langle e^{-\mathbf{r}^T A\mathbf{r}+s'^T\mathbf{r}}|e^{-\mathbf{r}^T B\mathbf{r}+s^T\mathbf{r}}\rangle \tag{4.7}$$

$$\langle G'^{(D)}|G^{(D)}\rangle = \left(\mathbf{a}^T\frac{\partial}{\partial s'^T}\right)\left(\mathbf{b}^T\frac{\partial}{\partial s'^T}\right)\left(\mathbf{c}^T\frac{\partial}{\partial s^T}\right)\left(\mathbf{d}^T\frac{\partial}{\partial s^T}\right)\langle e^{-\mathbf{r}^T A\mathbf{r}+s'^T\mathbf{r}}|e^{-\mathbf{r}^T B\mathbf{r}+s^T\mathbf{r}}\rangle \tag{4.8}$$

which is the expression that we want. We already know the analytic form of the overlap of shifted Gaussians, so inserting this in eq. (4.7) and eq. (4.8) we get

$$\langle G'^{(P)}|G^{(P)}\rangle = \left(\mathbf{a}^T\frac{\partial}{\partial s'^T}\right)\left(\mathbf{b}^T\frac{\partial}{\partial s^T}\right)e^{\frac{1}{4}(s+s')^T R(s+s')}\left(\frac{\pi^N}{det(A+B)}\right)^{3/2} \tag{4.9}$$

$$\langle G'^{(D)}|G^{(D)}\rangle = \left(\mathbf{a}^T\frac{\partial}{\partial s'^T}\right)\left(\mathbf{b}^T\frac{\partial}{\partial s'^T}\right)\left(\mathbf{c}^T\frac{\partial}{\partial s^T}\right)\left(\mathbf{d}^T\frac{\partial}{\partial s^T}\right)e^{\frac{1}{4}(s+s')^T R(s+s')}\left(\frac{\pi^N}{det(A+B)}\right)^{3/2} \tag{4.10}$$

In order to then get the overlap for the unshifted Gaussians, we can simple carry out the derivatives in eq. (4.9) and eq. (4.10) and then let $s, s' \to 0$.

$$\left(\mathbf{a}^T\frac{\partial}{\partial s^T}\right)\left(\mathbf{b}^T\frac{\partial}{\partial s'^T}\right)\langle e^{-\mathbf{r}^T A\mathbf{r}+s^T\mathbf{r}}|e^{-\mathbf{r}^T B\mathbf{r}+s'^T\mathbf{r}}\rangle \xrightarrow{s,s'\to 0} \langle g'^{(P)}|g^{(P)}\rangle \tag{4.11}$$

$$\left(\mathbf{a}^T\frac{\partial}{\partial s^T}\right)\left(\mathbf{b}^T\frac{\partial}{\partial s^T}\right)\left(\mathbf{c}^T\frac{\partial}{\partial s'^T}\right)\left(\mathbf{d}^T\frac{\partial}{\partial s'^T}\right)\langle e^{-\mathbf{r}^T A\mathbf{r}+s^T\mathbf{r}}|e^{-\mathbf{r}^T B\mathbf{r}+s'^T\mathbf{r}}\rangle \xrightarrow{s,s'\to 0} \langle g'^{(D)}|g^{(D)}\rangle \tag{4.12}$$

Doing this for the overlaps, we get.

$$\langle g'^{(P)}|g^{(P)}\rangle = \frac{1}{2}\left(\mathbf{a}^T R\mathbf{b}\right) M_0 \equiv M_1 \tag{4.13}$$

$$\langle g'^{(D)}|g^{(D)}\rangle = \frac{1}{4}\left(\left(\mathbf{a}^T R\mathbf{b}\right)\left(\mathbf{c}^T R\mathbf{d}\right) + \left(\mathbf{a}^T R\mathbf{b}\right)\left(\mathbf{c}^T R\mathbf{a}\right)\left(\mathbf{c}^T R\mathbf{b}\right)\left(\mathbf{d}^T R\mathbf{a}\right)\right) M_0 \equiv M_2 \tag{4.14}$$

where we remember that

$$M_0 = \left(\frac{\pi^N}{det(A+B)}\right)^{3/2} \tag{4.15}$$

where N now refers to the amount of spatial coordinates we use to describe our system. Notice that because the derivative with respect to the shift vectors is completely independent of the spatial coordinates, this method can also easily be generalized to overlaps with an operator in exactly the same way. As such, this method is a general method, applicable to all relevant components of the system.

We have written out the overlap of P- and D-wave Gaussians, but we still need to consider their overlap with the raising and lowering operator, along with the kinetic operator, $\hat{K}$. Considering the overlap with the raising and lowering operator, we can use the fact that W contains a Gaussian form factor, $f(r)$. Since the product of two Gaussians is another Gaussian, the general shape of the matrix elements will match the expressions in eq. (4.13) and eq. (4.14). One must just remember to multiply by the front factor S_W/b_W in eq. (3.9), and take into account that W adds the coordinate of the pion being created. The overlap with the kinetic energy operator is rather lengthy, and we refer to appendix C for the full shape of the matrix elements.

4.2 The One Pion subsystem

We consider the matrix element between two different Gaussian expansions, $\langle\psi^A_{N\pi}|\psi^B_{N\pi}\rangle$. Using the form of the wavefunctions derived in section 3.4, the one-pion overlap can be written as

$$\begin{aligned}&\langle\psi^{\alpha'}_{N\pi}|\psi^{\alpha}_{N\pi}\rangle = \\ &\langle e^{-\alpha' x^2}\frac{p\uparrow}{\sqrt{V}}(\bar{\tau}\bar{\pi})^\dagger(\bar{\sigma}\bar{x})^\dagger|(\bar{\tau}\bar{\pi})(\bar{\sigma}\bar{x})\frac{p\uparrow}{\sqrt{V}}e^{-\alpha r^2}\rangle\end{aligned} \tag{4.16}$$

We can use the identity $\left(\vec{\tau}\cdot\vec{\pi}\right)^\dagger\left(\vec{\tau}\cdot\vec{\pi}\right) = 3$, which is easily proven by explicit multiplication, to carry out the isospin part of the overlap. In order to deal with the spatial part of the overlap, we consider the spin part of the overlap.

$$\uparrow\left(\vec{\sigma}\cdot\vec{x}\right)\left(\vec{\sigma}\cdot\vec{x}\right)\uparrow = \uparrow|\left(\vec{\sigma}\cdot\vec{x}\right)(\uparrow\uparrow + \downarrow\downarrow)\left(\vec{\sigma}\cdot\vec{x}\right)\uparrow \tag{4.17}$$

where in the second expression, we have simply inserted the spin-space identity. Using the following two identities for applying spin to a Pauli vector,

$$\begin{aligned}\left(\vec{\sigma}\cdot\vec{x}\right)\uparrow &= \downarrow x + i\downarrow y + \uparrow z \\ \left(\vec{\sigma}\cdot\vec{x}\right)\downarrow &= \uparrow x - i\uparrow y - \downarrow z\end{aligned} \tag{4.18}$$

then, we can rewrite the left side of eq. (4.17).

$$\begin{aligned}&\uparrow\left(\vec{\sigma}\cdot\vec{x}\right)(\uparrow\uparrow + \downarrow\downarrow)\left(\vec{\sigma}\cdot\vec{x}\right)\uparrow = \uparrow\left(\vec{\sigma}\cdot\vec{x}\right)\uparrow\uparrow\left(\vec{\sigma}\cdot\vec{x}\right)\uparrow + \uparrow\left(\vec{\sigma}\cdot\vec{x}\right)\downarrow\downarrow\left(\vec{\sigma}\cdot\vec{x}\right)\uparrow \\ &= z^2 + (x - iy)(x + iy)\end{aligned} \tag{4.19}$$

where x, y, z are the three components of the relative coordinate vector, $\vec{r}$

$$\vec{r} = \begin{pmatrix} x \\ y \\ z \end{pmatrix} \tag{4.20}$$

Notice also, that $z^2 + (x - iy)(x + iy) = x^2 + y^2 + z^2 = r^2$, as one can also show by carrying out the product $\left(\vec{\sigma}\cdot\vec{r}\right)\left(\vec{\sigma}\cdot\vec{r}\right)$. We want to rewrite this into a form similar to what we derived in section 4.1. In the one-pion system, after a Jacobi transform, the vector $\mathbf{r}$ containing all the coordinates of our system only contains the relative coordinate between nucleon and pion.

$$\mathbf{r} = \vec{r} \tag{4.21}$$

Now, we define the three following vectors:

$$\mathbf{a} = \begin{pmatrix} 0 \\ 0 \\ 1 \end{pmatrix}, \quad \mathbf{b}_+ = \begin{pmatrix} 1 \\ i \\ 0 \end{pmatrix}, \quad \mathbf{b}_- = \begin{pmatrix} 1 \\ -i \\ 0 \end{pmatrix} \tag{4.22}$$

then we see that we can write

$$\left(\mathbf{a}^T r\right)\left(\mathbf{a}^T r\right) = z^2 \tag{4.23}$$

$$\left(\mathbf{b}_+{}^T r\right)\left(\mathbf{b}_-{}^T r\right) = x^2 + y^2 \tag{4.24}$$

which is just the sort of parametrization that we need, This means that we can write the matrix elements as follows.

$$\langle\psi^{\alpha}_{N\pi}|\psi^{\beta}_{N\pi}\rangle = 3\left(\langle e^{-\alpha r^2}|\left(\mathbf{a}^T\mathbf{r}\right)\left(\mathbf{a}^T\mathbf{r}\right)|e^{-\beta r^2}\rangle + \langle e^{-\alpha r^2}|\left(\mathbf{b}_+{}^T\mathbf{r}\right)\left(\mathbf{b}_-{}^T\mathbf{r}\right)|e^{-\beta r^2}\rangle\right) \tag{4.25}$$

which also generalizes to the kinetic energy terms. These terms can no be applied directly to the matrix elements that were derived in section 4.1.

4.3 The Two-Pion Subsystem

The approach to solving the two-pion system follows much the same procedure, but the added complexity of the second pion means that some hurdles have to be managed. The overlap between the two-pion wavefunctions, $\langle\psi^A_{N\pi\pi}|\psi^B_{N\pi\pi}\rangle$ written in relative Jacobi coordinates $\mathbf{x}$ is as follows.

$$\begin{aligned}&\langle\psi^A_{N\pi\pi}|\psi^B_{N\pi\pi}\rangle = \\ &\langle e^{-\mathbf{x}^T A\mathbf{x}}\frac{p\uparrow}{\sqrt{V}}\left(\vec{\tau}\cdot\vec{\pi}_1\right)^\dagger\left(\vec{\sigma}\cdot\vec{x}_1\right)^\dagger\left(\vec{\tau}\cdot\vec{\pi}_2\right)^\dagger\left(\vec{\sigma}\cdot\vec{x}_2\right)^\dagger|\left(\vec{\tau}\cdot\vec{\pi}_2\right)\left(\vec{\sigma}\cdot\vec{x}_2\right)\left(\vec{\tau}\cdot\vec{\pi}_1\right)\left(\vec{\sigma}\cdot\vec{x}_1\right)\frac{p\uparrow}{\sqrt{V}}e^{-\mathbf{x}^T B\mathbf{x}}\rangle\end{aligned} \tag{4.26}$$

Carrying out the product of $\left(\vec{\tau}\cdot\vec{\pi}_i\right)^\dagger\left(\vec{\tau}\cdot\vec{\pi}_i\right)$ for both the first and second pion, we can rewrite eq. (4.26).

$$\begin{aligned}&\langle\psi^A_{N\pi\pi}|\psi^B_{N\pi\pi}\rangle = \\ &9\langle e^{-\mathbf{x}^T A\mathbf{x}}\frac{\uparrow}{\sqrt{V}}\left(\vec{\sigma}\cdot\vec{x}_1\right)^\dagger\left(\vec{\sigma}\cdot\vec{x}_2\right)^\dagger|\left(\vec{\sigma}\cdot\vec{x}_2\right)\left(\vec{\sigma}\cdot\vec{x}_1\right)\frac{\uparrow}{\sqrt{V}}e^{-\mathbf{x}^T B\mathbf{x}}\rangle\end{aligned} \tag{4.27}$$

As with the one-pion case, we consider just the spin part of the wavefucntion. Inserting the spin-space identity in eq. (4.27)

$$\begin{aligned}&\uparrow\left(\vec{\sigma}\cdot\vec{x}_1\right)^\dagger\left(\vec{\sigma}\cdot\vec{x}_2\right)^\dagger\left(\vec{\sigma}\cdot\vec{x}_2\right)\left(\vec{\sigma}\cdot\vec{x}_1\right)\uparrow= \\ &\uparrow\left(\vec{\sigma}\cdot\vec{x}_1\right)^\dagger(\uparrow\uparrow+\downarrow\downarrow)\left(\vec{\sigma}\cdot\vec{x}_2\right)^\dagger(\uparrow\uparrow+\downarrow\downarrow)\left(\vec{\sigma}\cdot\vec{x}_2\right)(\uparrow\uparrow+\downarrow\downarrow)\left(\vec{\sigma}\cdot\vec{x}_1\right)\uparrow\end{aligned} \tag{4.28}$$

We now carry out the sum of terms in eq. (4.28) using the identities in eq. (4.18). They take much the same form as the elements we derived in section 4.2, but the addition of the second pion increases the complexity of the task considerably. We get 8 terms, and they take the form.

$$\begin{aligned}&\uparrow\left(\vec{\sigma}\cdot\vec{x}_1\right)^T\left(\vec{\sigma}\cdot\vec{x}_2\right)^T\left(\vec{\sigma}\cdot\vec{x}_2\right)\left(\vec{\sigma}\cdot\vec{x}_1\right)\uparrow \\ &=(\vec{e}_z\cdot\vec{x}_1)(\vec{e}_z\cdot\vec{x}_2)(\vec{e}_z\cdot\vec{x}_2)(\vec{e}_z\cdot\vec{x}_1) \\ &+(\vec{e}_z\cdot\vec{x}_1)(\vec{e}_z\cdot\vec{x}_2)(\vec{e}_+\cdot\vec{x}_2)(\vec{e}_-\cdot\vec{x}_1) \\ &+(\vec{e}_z\cdot\vec{x}_1)(\vec{e}_+\cdot\vec{x}_2)(\vec{e}_-\cdot\vec{x}_2)(\vec{e}_z\cdot\vec{x}_1) \\ &-(\vec{e}_z\cdot\vec{x}_1)(\vec{e}_+\cdot\vec{x}_2)(\vec{e}_z\cdot\vec{x}_2)(\vec{e}_-\cdot\vec{x}_1) \\ &+(\vec{e}_+\cdot\vec{x}_1)(\vec{e}_-\cdot\vec{x}_2)(\vec{e}_z\cdot\vec{x}_2)(\vec{e}_z\cdot\vec{x}_1) \\ &+(\vec{e}_+\cdot\vec{x}_1)(\vec{e}_-\cdot\vec{x}_2)(\vec{e}_+\cdot\vec{x}_2)(\vec{e}_-\cdot\vec{x}_1) \\ &-(\vec{e}_+\cdot\vec{x}_1)(\vec{e}_z\cdot\vec{x}_2)(\vec{e}_-\cdot\vec{x}_2)(\vec{e}_z\cdot\vec{x}_1) \\ &+(\vec{e}_+\cdot\vec{x}_1)(\vec{e}_z\cdot\vec{x}_2)(\vec{e}_z\cdot\vec{x}_2)(\vec{e}_-\cdot\vec{x}_1)\end{aligned} \tag{4.29}$$

where

$$\vec{e}_z=\begin{pmatrix}0\\0\\1\end{pmatrix},\quad \vec{e}_+=\begin{pmatrix}1\\i\\0\end{pmatrix},\quad \vec{e}_-=\begin{pmatrix}1\\-i\\0\end{pmatrix}, \tag{4.30}$$

This leaves us with just the spatial terms and the overlap of the Gaussians to consider. Let us consider the overlap of Gaussians with a single general term in eq. (4.29). We consider general unit vectors labeled $\vec{e}_{\delta,\gamma,\nu,\mu}$, which are similar to the unit vectors in eq. (4.30). Additionally, using the notation $\vec{x}_i = w_i^T \mathbf{x}$, we can write

$$\langle e^{-\mathbf{x}^T B \mathbf{x}} \left[\vec{e}_\delta (w_1^T \mathbf{x})\right] \left[\vec{e}_\gamma (w_2^T \mathbf{x})\right] \left[\vec{e}_\mu (w_2^T \mathbf{x})\right] \left[\vec{e}_\nu (w_1^T \mathbf{x})\right] e^{-\mathbf{x}^T A \mathbf{x}} \rangle \tag{4.31}$$

We can split open the parenthesis in the hard brackets in eq. (4.31) and consider the product of the unit vectors with the vectors w. This gives us vectors, with a unit vector entry, which we label.

$$\mathbf{a} = \left(\vec{e}_\delta w_1\right) = \begin{pmatrix} \vec{e}_\delta \\ 0 \\ 0 \end{pmatrix}, \quad \mathbf{b} = \left(\vec{e}_\gamma w_2\right) = \begin{pmatrix} 0 \\ \vec{e}_\gamma \\ 0 \end{pmatrix}, \quad \mathbf{c} = \left(\vec{e}_\mu w_1\right) = \begin{pmatrix} \vec{e}_\mu \\ 0 \\ 0 \end{pmatrix}, \quad \mathbf{d} = \left(\vec{e}_\nu w_2\right) = \begin{pmatrix} 0 \\ \vec{e}_\nu \\ 0 \end{pmatrix}, \tag{4.32}$$

such that the final form of the overlap terms in eq. (4.31) becomes

$$\begin{aligned} &\langle e^{-\mathbf{x}^T B \mathbf{x}} \left[\vec{e}_\delta (w_1^T \mathbf{x})\right] \left[\vec{e}_\gamma (w_2^T \mathbf{x})\right] \left[\vec{e}_\mu (w_2^T \mathbf{x})\right] \left[\vec{e}_\nu (w_1^T \mathbf{x})\right] e^{-\mathbf{x}^T A \mathbf{x}} \rangle = \\ &\langle e^{-\mathbf{x}^T B \mathbf{x}} \left(\mathbf{a}^T \mathbf{x}\right) \left(\mathbf{b}^T \mathbf{x}\right) \left(\mathbf{c}^T \mathbf{x}\right) \left(\mathbf{d}^T \mathbf{x}\right) e^{-\mathbf{x}^T A \mathbf{x}} \rangle \end{aligned} \tag{4.33}$$

So each term in eq. (4.29) can be written in our general form eq. (4.31), and a matrix element is calculated for each. Notice aswell that the shape of any of the vectors in eq. (4.32) are unaffected by the Jacobi transform. As an example, consider $\mathbf{a}^T \mathbf{x}$. Using that $\mathbf{x} = J\mathbf{r}$ and $w \to U^T w$, where $U = J^{-1}$

$$\mathbf{a}^T \mathbf{x} = \left(\vec{e}_\delta \left(U^T w_1\right)^T J \mathbf{r}\right) = \left(\left(\vec{e}_\delta w_1\right)^T U J \mathbf{r}\right) = \left(\left(\vec{e}_\delta w_1\right) \mathbf{r}\right) = \left(\mathbf{a}^T \mathbf{r}\right) \tag{4.34}$$

So this general expansion method works no matter the coordinate system that is considered.

4.4 Alternative Methods for Calculating Matrix Elements

The expansion method we considered in section 4.1 becomes rather lengthy, even for the expansion of the D-wave matrix elements. Let us therefore discuss other methods that can be used to calculate the matrix elements. Some of these methods were considered for usage in this thesis, but certain complications halted their usage.

If we begin by considering the one-pion system, we remember from eq. (3.39) that the wavefunction can be written as

$$\psi_{\tilde{N}\pi\pi} = \left(\vec{\tau} \cdot \vec{\pi}\right) \left(\vec{\sigma} \cdot \vec{r}\right) \sum_{i=1}^{n_g} c_i e^{-\alpha_i r^2}$$

Noticeably, there is only one coordinate in this expansion, and so the matrix elements between one-pion wavefunction are easily carried out by explicit integration. We will not go into detail here, but refer to [7] for the matrix elements calculated using this method.

For the two pion system, explicit integration is not an option. The addition of the extra coordinate, along with their coupling through off-diagonal terms in the parameter matrix, makes it unfeasible to calculate the integral. However, the overlap can be calculated in quite an ingenious way. This method follows many of the same ideas that were discussed in section 4.1, and involves taking the derivative of the diagonal elements of the parameter matrices, A in the two-pion wavefunction similar to eq. (3.53). Let us first consider the two pion wavefunction

$$\psi_{\tilde{N}\pi\pi} = \left(\vec{\tau}\cdot\vec{\pi}_1\right)\left(\vec{\sigma}\cdot\vec{x}_1\right)\left(\vec{\tau}\cdot\vec{\pi}_2\right)\left(\vec{\sigma}\cdot\vec{x}_2\right)\sum_{i=1}^{n_g} c_i e^{-\mathbf{x}^T A_i \mathbf{x}}$$

Taking the overlap of the two pion wavefunction with itself and considering a single term in the sum, we can use the identity $\left(\vec{\sigma}\cdot\vec{x}\right)\left(\vec{\sigma}\cdot\vec{x}\right) = x^2$ to write

$$\begin{aligned}&\langle e^{-\mathbf{x}^T A\mathbf{x}}|\left(\vec{\tau}\cdot\vec{\pi}_1\right)^\dagger\left(\vec{\sigma}\cdot\vec{x}_1\right)^\dagger\left(\vec{\tau}\cdot\vec{\pi}_2\right)^\dagger\left(\vec{\sigma}\cdot\vec{x}_2\right)^\dagger\left(\vec{\tau}\cdot\vec{\pi}_2\right)\left(\vec{\sigma}\cdot\vec{x}_2\right)\left(\vec{\tau}\cdot\vec{\pi}_1\right)\left(\vec{\sigma}\cdot\vec{x}_1\right)|e^{-\mathbf{x}^T B\mathbf{x}}\rangle \\ &= 9\langle e^{-\mathbf{x}^T A\mathbf{x}}|x_1^2x_2^2|e^{-\mathbf{x}^T B\mathbf{x}}\rangle\end{aligned} \tag{4.35}$$

where we have also used $\left(\vec{\tau}\cdot\vec{\pi}\right)\left(\vec{\tau}\cdot\vec{\pi}\right) = 3$. We now want to consider the Gaussians themselves. The rightmost Gaussian in eq. (4.35) containts the terms B, which is a 2×2 parameter matrix, and $\mathbf{x}$, a vector of size 2 with 3-dimensional coordinate vectors in each entry. Writing out the terms we get an ordinary one-dimensional number

$$-\mathbf{x}^T B\mathbf{x} = -B_{11}x_1^2 - B_{22}x_2^2 - 2B_{12}\vec{x}_1\cdot\vec{x}_2 \tag{4.36}$$

where B_{ij} is the $i,j'th$ entry in the matrix B. Notice that we have written $2B_{12}$, since the matrix B is symmetric, so $B_{21} = B_{12}$. Taking the derivatives of the Gaussian $e^{-\mathbf{x}^T B\mathbf{x}}$ with respect to the diagonal elements

$$\frac{\partial}{\partial B_{11}}\frac{\partial}{\partial B_{22}}e^{-\mathbf{x}^T B\mathbf{x}} = x_1^2x_2^2e^{-\mathbf{x}^T B\mathbf{x}} \tag{4.37}$$

which then suggests that we can write the matrix element in eq. (4.35) as

$$\begin{aligned}\langle e^{-\mathbf{x}^T A\mathbf{x}}|x_1^2x_2^2|e^{-\mathbf{x}^T B\mathbf{x}}\rangle &= \frac{\partial}{\partial B_{11}}\frac{\partial}{\partial B_{22}}\langle e^{-\mathbf{x}^T A\mathbf{x}}|e^{-\mathbf{x}^T B\mathbf{x}}\rangle \\ &= \frac{\partial}{\partial B_{11}}\frac{\partial}{\partial B_{22}}\left(\frac{\pi^2}{det(A+B)}\right)^{3/2}\end{aligned} \tag{4.38}$$

Carrying out this derivative is pretty straight forward once the determinant is written out explicitly. The final matrix element then takes the form

$$\begin{aligned}\langle e^{-\mathbf{x}^T A\mathbf{x}}|x_1^2 x_2^2|e^{-\mathbf{x}^T B\mathbf{x}}\rangle &= \frac{\partial}{\partial B_{11}}\frac{\partial}{\partial B_{22}}\left(\frac{\pi^2}{det(A+B)}\right)^{3/2} \\ &= \frac{3\pi^3}{4}\frac{3C_{11}C_{22}+2C_{12}^2}{det(C)^{7/2}}\end{aligned} \tag{4.39}$$

where

$$C = A + B \tag{4.40}$$

and C_{ij} are the matrix entries in the matrix C. This method of calculating matrix elements has a lot of benefits compared to the general expansion method used in section 4.1. It is much easier to calculate analytically than the general method, and we don't have to concern ourselves with the spin structure explicitly. It can also be easily generalized to higher order systems. If we consider some system with N-particles having the position vector $\mathbf{r}$ of length N and A, B being $N \times N$ matrices

$$\langle e^{-\mathbf{r}^T A\mathbf{r}}|r_1^2 r_2^2 \dots r_N|e^{-\mathbf{r}^T B\mathbf{r}}\rangle = \left((-1)^N \prod_{i=1}^{N}\frac{\partial}{\partial B_{ii}}\right)\langle e^{-\mathbf{r}^T A\mathbf{r}}|e^{-\mathbf{r}^T B\mathbf{r}}\rangle \tag{4.41}$$

that is, take the derivatives of all the diagonal elements of the known matrix element $\langle e^{-\mathbf{r}^T A\mathbf{r}}|e^{-\mathbf{r}^T B\mathbf{r}}\rangle$, and multiply by a factor $(-1)^N$, which must be included to account for the sign in $-\mathbf{r}B\mathbf{r}$.

This method seemingly allows easy generalization to higher order pion approximations. The problem standing in the way of this method is the kinetic term. Writing out the two-pion matrix element for the kinetic operator in its spatial coordinates

$$\langle e^{-\mathbf{x}^T A\mathbf{x}}|\left(\vec{\sigma}\cdot\vec{x}_1\right)^\dagger\left(\vec{\sigma}\cdot\vec{x}_2\right)^\dagger\hat{K}\left(\vec{\sigma}\cdot\vec{x}_2\right)\left(\vec{\sigma}\cdot\vec{x}_1\right)|e^{-\mathbf{x}^T B\mathbf{x}}\rangle \tag{4.42}$$

But the coordinate terms do not commute with the kinetic operator, and so we cannot write the kinetic matrix element in a similar fashion as eq. (4.38). An initial idea would be to use the identity

$$\left(\vec{\sigma}\cdot\vec{x}_2\right)\left(\vec{\sigma}\cdot\vec{x}_1\right) = \left(\vec{x}_2\cdot\vec{x}_1\right)I + i\left(\vec{x}_2\times\vec{x}_1\right)\cdot\vec{\sigma} \tag{4.43}$$

with I being the identity, such that eq. (4.42) can be written on the form

$$\langle e^{-\mathbf{x}^T A\mathbf{x}}|\left[\left(\vec{x}_1\cdot\vec{x}_2\right)I + i\left(\vec{x}_1\times\vec{x}_2\right)\cdot\vec{\sigma}\right]\hat{K}\left[\left(\vec{x}_2\cdot\vec{x}_1\right)I + i\left(\vec{x}_2\times\vec{x}_1\right)\cdot\vec{\sigma}\right]|e^{-\mathbf{x}^T B\mathbf{x}}\rangle \tag{4.44}$$

From eq. (4.44), we note that the term involving just the dot product between $\vec{x}_1\cdot\vec{x}_2$ can be solved using a similar method to what we did for the overlap. Instead of taking the derivative with respect to the diagonal terms, we now do it with respect to the off-diagonal terms.

$$\langle e^{-\mathbf{x}^T A\mathbf{x}}| \left(\vec{x}_1 \cdot \vec{x}_2\right) \hat{K} \left(\vec{x}_2 \cdot \vec{x}_1\right) |e^{-\mathbf{x}^T B\mathbf{x}}\rangle = \frac{1}{2}\frac{\partial}{\partial A_{12}}\frac{1}{2}\frac{\partial}{\partial B_{12}}\langle e^{-\mathbf{x}^T A\mathbf{x}}|\hat{K}|e^{-\mathbf{x}^T B\mathbf{x}}\rangle \tag{4.45}$$

However, the remaining terms involves the cross product of the two vectors in some way, and the only apparent way forward is explicit integration, which quickly becomes a complicated process. Alternatively, one can supplement the general expansion method for the kinetic term with the method in eq. (4.38) for the overlaps, but applying the general method to kinetic matrix elements is already a lengthy process, as appendix C is a clear example of. As such, the general expansion method has been the method of choice when doing numerical calculations on the pion dressing.

Chapter 5

Results

In this section, we use the matrix elements we found in chapter 4 to investigate the effect of the second pion in the dressing of the nucleon. We begin by considering the single pion dressing, which serves as a proof of concept for the general theory. We will compare the Gaussian solution, eq. (3.39), of the one pion dressing with a direct solution of a coupled differential equation, which yields the same answer. Next, we investigate the dressing of two pions. We document the effect of the second pion at different coupling parameters, S_W and b_W, and discuss the boundaries for where the one pion approximation is sufficient, and when the two pion system needs to be included.

5.1 One-pion dressing

In the one pion dressing, we solve the Schrödinger equation in eq. (3.33) using the matrix elements derived in section 4.2. We have chosen the coupling parameters $S_W = 41.5MeV$ and $b_W = 3.9fm$, which was found to be the ideal set of parameters to describe neutral pion photoproduction off protons [7]. For each Gaussian, we remember to subtract the energy, $\tilde{E}$ from the mass of the physical proton, $\check{m}_N$ in order to get the correct mass of the bare nucleon, $\check{m}_{\tilde{N}}$. In practice, we do as follows for each Gaussian added to the system: First, we solve the system under the condition $\check{m}_{\tilde{N}} = \check{m}_N$, giving us the energy $\tilde{E}_0$. We then run a second iteration with the same Gaussian, now using $\check{m}'_{\tilde{N}} = \check{m}_N - \tilde{E}_0$, giving us the energy $\tilde{E}_1$, repeating the process with this new energy. We will run these iterations 2-3 times in order to ensure a good convergence towards the correct result.

The Gaussian solution will be compared to a different method, where eq. (3.33) can be solved as an initial value problem. The details are omitted in this thesis, but we refer to [20] for a complete walk through of this method. The convergence for the Gaussian method towards the solution of the coupled system can be seen in figure 5.1.

We see in fig. 5.1 that the Gaussian method converges toward the final value of the system after only one to two Gaussians. This is a bit surprising, since other

simple systems typically take 4-5 Gaussians to fully converge, see appendix B. A possible explanation is the Gaussian shape of the coupling potential, eq. (3.9). The Gaussian form factor can be seen as the inhomogenous term in the set of coupled differential equations we considered in eq. (3.34) and eq. (3.35). The kinetic terms are the homogenous terms, but since the pion is under barrier, a possible explanations is that the wavefunction follows the larger coupling term, which is also a Gaussian, and shapes itself after that.

The final state energies achieved are consistent with [7], and the Gaussian solution matches the direct solution to the initial value problem. Even with just a single Gaussian, the convergence towards the final solution is very good, and the only discrepancies that are noticeable arise when we zoom in to a part of the graph. Even so, the difference is minimal, and a good result for the one pion dressing can easily be obtained using just a single Gaussian.

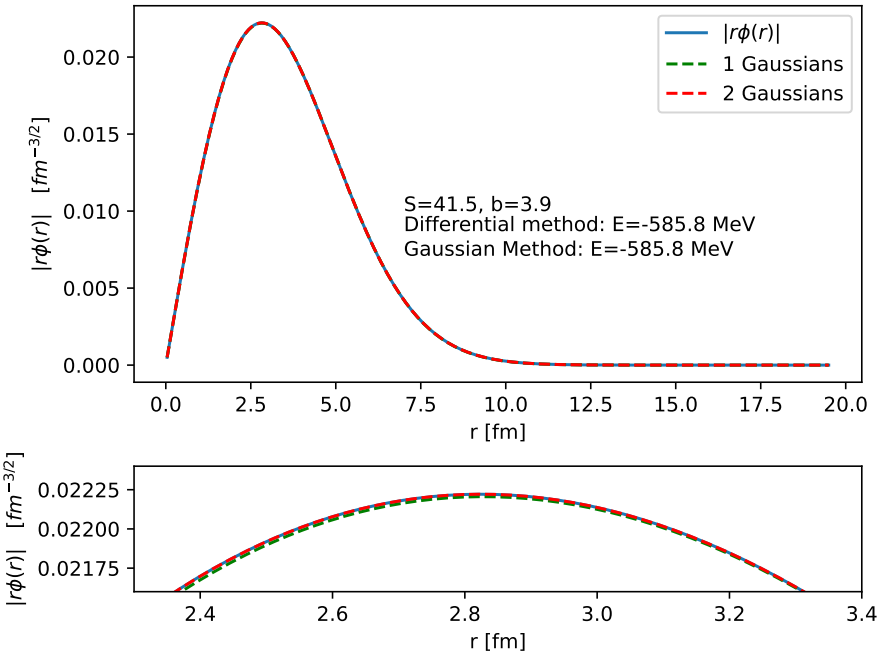

FIGURE 5.1: The absolute value of the radial wave function for the dressing of the proton with a single pion. The system is solved both using Gaussians and by the solving an initial value problem numerically. The parameters used for the coupling are $S_W = 41.5MeV$ and $b_W = 3.9fm$. The lower graph shows a zoomed in section of the graph. We see the convergence towards the differential solution is excellent after only a single Gaussian, while two Gaussians is a near perfect solution.

5.2 Comparing the One and the Two Pion Approximation.

The addition of the second pion means that the potential barrier of which the pions are under is doubled. It can therefore be expected that the first pion has the biggest

contribution to the dressing of the proton, given that it is under a smaller barrier. As such, we expect to see a decrease in the ground state energy of the entire system, but the decrease shouldn't be as drastic as with the addition of the first pion. The convergence towards the energy of the two-pion dressing can be seen in fig. 5.2. We have used the same parameters as in section 5.1 so as to more easily compare the differences and similarities. For each system, we have used 3 Gaussian so as to see how they converge toward their final state energies.

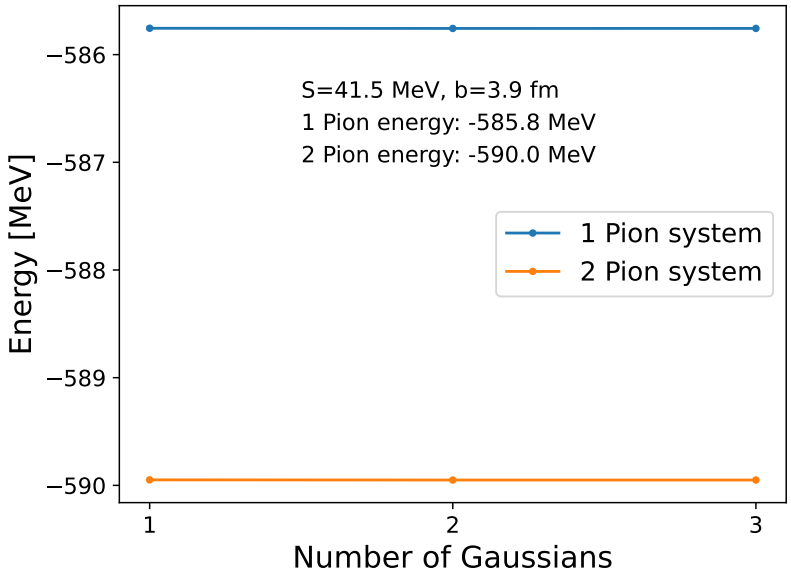

FIGURE 5.2: The convergence toward the final state energy of the one and the two pion system as a function of the number of Gaussians used. The coupling parameters used are $S_W = 41.5MeV$ and $b_W = 3.9fm$. The blue line is the energy from the nucleon dressed by a single pion, while the orange line is the energy convergence for the nucleon dressed by two pions. 3 Gaussians have been used in each case. The difference in energy is roughly $4MeV$. We see that the convergence towards the final state energy happens almost immediatly, with no notable change when the second Gaussian is added.

As fig. 5.2 shows, we see much the same picture as we did in fig. 5.1, with the addition of multiple Gaussians not making a significant difference in the dressing energy of the systems. This is good news for the model, since using fewer Gaussians drastically cuts down on the computation time of the system, which is especially the case for the two pion system, which requires the optimization of three parameters for each Gaussian used. As such, we will assume unless otherwise specified, that future simulations have been performed using a single D-wave Gaussian for the two pion system.

As expected, the first pion has a much higher contribution to the dressing of the proton. The final state energy in the dressing of the second Pion is about $-590MeV$, which is a difference of about $4MeV$ from the energy of the one-pion system. Such an energy difference may or may not prove significant depending on the level of precision we might need, but to simulate tendencies, the one pion system should be

sufficient at these parameters. This graph is of course not conclusive, as we have only shown the difference in the energies for a single value of the coupling parameters. For a more complete picture of the effect of the second pion, we must therefore investigate its effect at different coupling parameters.

5.2.1 Variation in coupling strength.

In order to investigate the coupling fully, we compare the differences of the two systems at different couplings strengths, S_W, from equation 3.9. This is shown in fig. 5.3, where we plot the contribution to the norm of the wavefunction as a function of the coupling strength, S_W. For this purpose, we have set $b_W = 3fm$ for all possible variations in the coupling strength. As we increase the coupling strength, we expect the contribution from the bare nucleon to fall, while the contribution from the first and the second pion increases, due to the increased coupling strength.

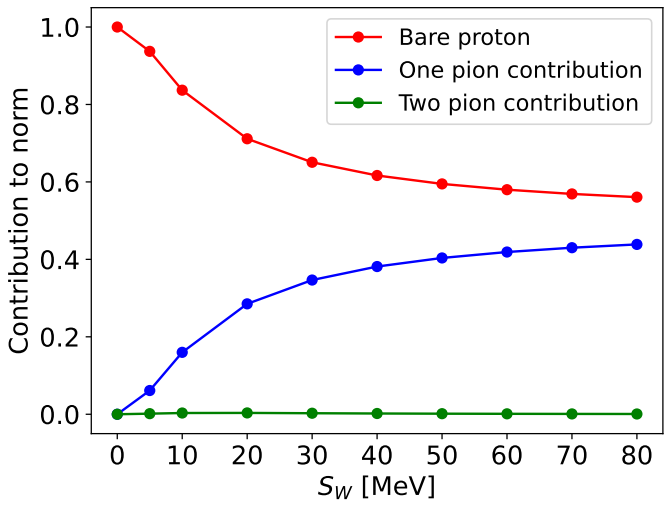

FIGURE 5.3: The contribution to the norm of the different systems as a function of coupling strength. The range parameter has been fixed at $b_W = 3fm$. At low coupling strengths, the system is dominated by the bare proton, but as S_W increases, the one pion contribution starts to increase, reaching a similar level to the bare proton system. The two pion system stays flat at all values of S_W, which indicates that only the one pion system benefits from increases in coupling strength.

We discussed the normalization of the wavefunction of the two-pion system in section 3.4, where we required that the total wavefunction be normalized to unity, as was demonstrated in eq. (3.41). We can also write eq. (3.41) in terms of our Gaussian expansion. In eq. (2.8), we noted how we could write the norm of the wavefunction as a matrix equation using the eigenvectors, c and the overlap matrix $\mathcal{N}$.

$$|\Psi_2|^2 = c^T \mathcal{N} c = 1 \tag{5.1}$$

where $\mathcal{N}$ is parameterized according to eq. (3.55). In order to then get the contribution from each part of the system, we can simply calculate the product of each block along the diagonal with their respective eigenvectors.

$$c^T \mathcal{N} c = c^T_{\tilde{N}} \mathcal{N}_{\tilde{N}} c_{\tilde{N}} + c^T_{\tilde{N}\pi} \mathcal{N}_{\tilde{N}\pi} c_{\tilde{N}\pi} + c^T_{\tilde{N}\pi\pi} \mathcal{N}_{\tilde{N}\pi\pi} c_{\tilde{N}\pi\pi} \tag{5.2}$$

with the subscripts indicating which system we consider in each term.

When the coupling strength is 0, the systems are completely uncoupled, and we consider just a bare nucleon. Naturally, this means the contribution to the norm of the wavefunction resides entirely with the bare nucleon system. As the coupling strength increases, so does the contribution from the one-pion system. We see that as the coupling strength increases, the contribution of the first pion increases while the contribution from the bare proton starts decreasing. This is completely as expected. One might even expect that if the coupling strength is increased further, that the one-pion contribution would surpass the bare proton contribution and become the dominating contribution.

Looking at the two-pion system however, we see that its contribution stays flat compared to the trajecetory of the other two systems. The apparent contribution of the second pion is so small, that the changes aren't visible in fig. 5.3. In order to get a better understanding of the contribution of the second pion, we plot its contribution to the norm of the wavefunction separately. This can be seen in fig. 5.4.

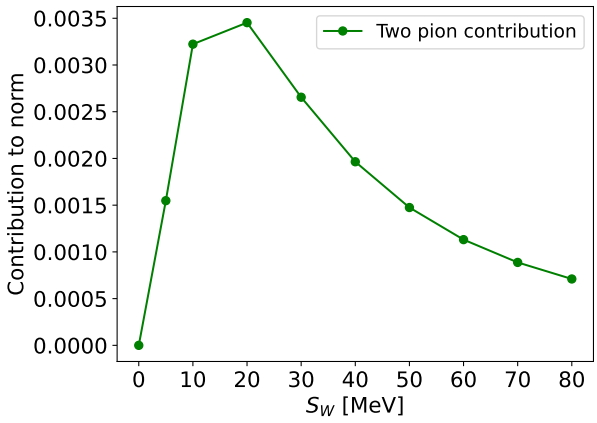

FIGURE 5.4: Contribution from the second pion to the total norm of the wavefunction as a function of coupling strength. The range parameter has been fixed at $b_W = 3fm$. We see an initial increase in the system's contribution to the norm, but when $S_W = 20Mev$, the contribution starts dropping off again.

The two pion system's total contribution peaks at about 0.35% at around $10 - 20MeV$. What is maybe a bit surprising is that the contribution to the norm of the wavefunction starts falling again when the coupling strength is increased beyond $20MeV$. A possible explanation is the stronger coupling of the first pion compared to that of the second pion. Since the first pion is more strongly bound to the proton, an increase in coupling strength might only benefit the first and more tightly bound pion. This is further backed up by what we saw in fig. 5.3, as the one pion contribution to the norm increases even at larger values of S_W. This appears to be at the detriment of the two pion contribution.

We can also consider the relative difference in final state energies as a function of coupling strength. We plot the value

$$\Delta_{E_{rel}} = \frac{|E_2 - E_1|}{|E_2|} \tag{5.3}$$

where E_2 is the energy of the two pion system and E_1 is the energy of the one pion system, as a function of the coupling strength. This gives us an idea of how the two systems grow compared to eachother. This can be seen in fig. 5.5.

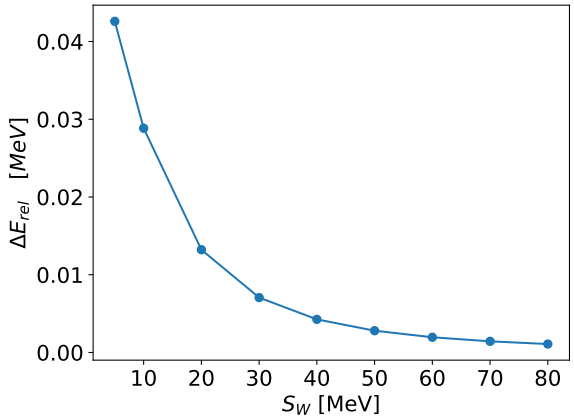

FIGURE 5.5: The relative energy difference between the one pion and the two pion systems as a function of coupling strength. The range parameter has been fixed at $b_W = 3fm$. The relative energy difference between the two systems starts at around 4% but drops all the way toward 0% when the coupling strength is large.

We see that when the coupling strength is low, the relative difference is about 4%, but it falls exponentially with increasing coupling strength. This tells us that as S_W increases, the one pion contribution will remain the dominating contribution of the two different pion systems, and that the two pion contribution will continue to be irrelevant, even as S_W is increased.

5.2.2 Variation in coupling range

Next, we compare how varying the range of the interaction, the parameter b_W, affects the contribution of the second pion. For this purpose, we keep S_W fixed at $20MeV$, which proved to be the coupling strength with the largest contribution for the two-pion overlap. We investigate how the contribution varies with different values of b_W. Since the pion interactions are responsible for the long range interaction of the nuclear force, we should expect the contribution from the pion systems to increase with increasing b_W [3]. This can also be gathered from the e^{-r^2/b_W} term in the coupling factor, eq. (3.9), where and increase in b_W will lead to a larger coupling parameter. However, since the coupling strength grows as e^{-1/b_W}, we would also expect the growth in contribution to taper of a bit when b_W is increased considerably.

We begin by considering the contribution of the different systems to the norm as a function of b_W. This can be seen in fig. 5.6.

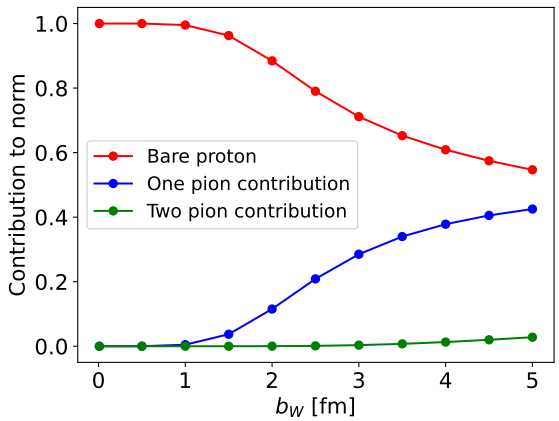

FIGURE 5.6: The contribution to the norm of the wavefunction for the different parts of the system as a function of the range parameter, b_W. The coupling strength has been fixed at a value of $S_W = 20MeV$. We see both of the pion systems having low contributions when b_W is low, where the bare proton system dominates. As b_W increases, we see a noticeable rise in the one-pion contribution. We also see a slight increase in the contribution for the two pion system when b_W is large.

The first notable difference between the variation of the coupling strength and the variation of the coupling range is that the contribution from either of the two pions systems is practically zero until b_W reaches a value of around $1.5fm$. From this point, the contribution from the first pion begins to increase, while the contribution from the bare proton starts dropping. When b_W is low, the exponential term, $e^{-\frac{1}{b_W^2}r^2}$, suppresses the strength of the coupling. However, as b_W increases, the exponential term becomes more dominating, and the contribution to the one pion system increases. A primary difference from when the coupling strength was varied is that the two pion contribution is now notable, as can be seen in fig. 5.7.

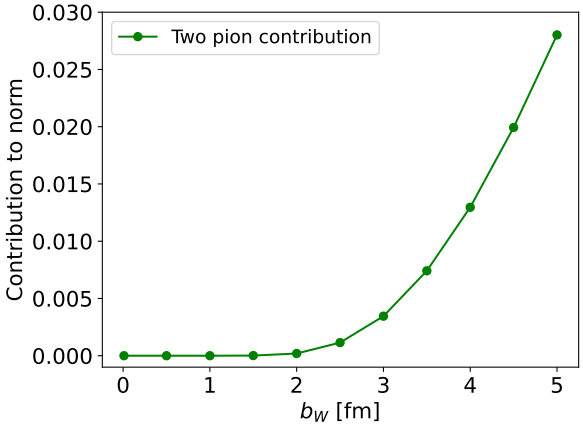

FIGURE 5.7: Contribution from the second pion to the total norm of the wavefunction as a function of the range parameter. The coupling strength has been fixed at a value of $20MeV$. When the range parameter is low, we see no contribution from the two pion system, but around when $b_W = 2fm$, the contribution begins to increase drastically, reaching above 2.5% for the values we have plotted.

Whereas before the contribution from the second pion was more or less totally insignificant, this is not so the case anymore. Since the strength of the interaction is now driven by the exponential term instead of the linear front factor, $\frac{S_W}{b_W}$ in eq. (3.9), we see an increase in the contribution from the second pion as b_W increases. For the range parameters considered in fig. 5.7, this amounts to a little over 2.5% of the total contribution. While this is still a small contribution compared to the bare nucleon system and the one pion system, it might prove significant depending on the level of accuracy one requires. On top of this, let us compare the relative energy differences between the one and the two pion system, in fig. 5.8.

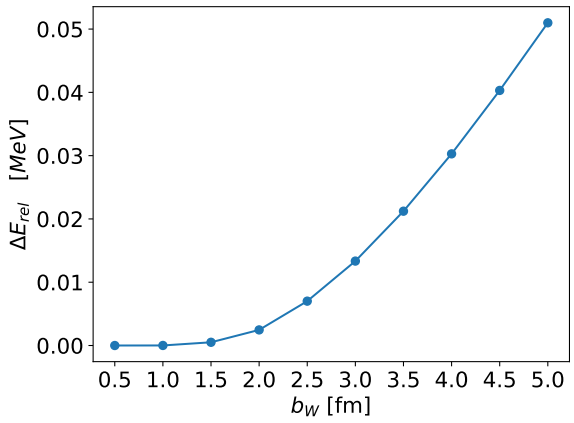

FIGURE 5.8: Relative energy difference between the one pion and the two pion system as a function of the coupling range, b_W. The coupling strength has been fixed at a value of $S_W = 20MeV$. Similarly to fig. 5.7, the influence of the two pion system can be seen to increase exponentially.

Now, the relative difference increases with increasing b_W, which shows an increase in influence from the two pion. The peak relative energy difference between the two systems is at about 5% for the values of b_W considered in fig. 5.8, which corresponds to a total energy difference of around $20MeV$.[1] This is a significant difference, but the one pion approximation still gives reasonably good results even at this coupling range. Seeing as the relative contribution from the two pion system increases with b_w, the next natural step is to consider what happens if we turn up b_W even more. This can be seen in fig. 5.9, where we consider coupling ranges up to $9fm$.

The first thing we can notice in fig. 5.9 is that the one pion contribution becomes the dominating contribution to the total norm, with it crossing the contribution to the norm of the bare proton. Notice also however that this increase is not due to a drastic increase in the contribution from the first pion. In fact, the contribution from the first pion never reaches beyond 50%. Rather, it is a drop in the contribution from the bare proton, which then leads to a subsequent increase in the contribution from the second pion. We see a drastic increase in the two pion contribution, which reaches contributions of the total norm up to 10% and still increasing. The two pion contribution can no longer be disregarded, and must be included to give a proper description of the system.

1: The energy of the two pion system at this relative energy difference is around $-414MeV$.

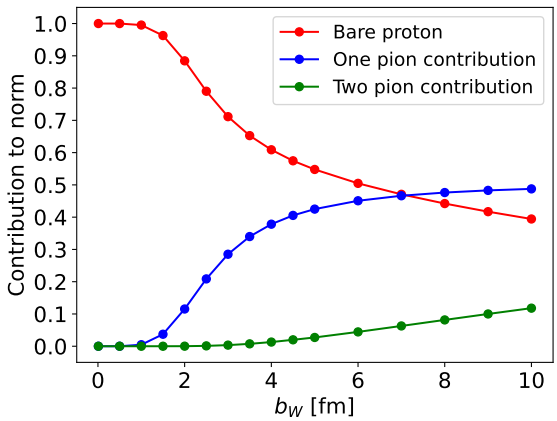

FIGURE 5.9: Contributions to the total norm for different parts of the total wavefunction for high values of b_W. The coupling strength has been set to a value of $S_W = 20MeV$. We see a continuation of the tendencies we originally saw in fig. 5.6, with the one pion contribution crossing the contribution from the bare nucleon. We also see a notable increase in the two pion contribution.

We also see that while the the one pion contribution is still increasing, it does so at a lower rate than compared to smaller values of b_W. This is in no doubt due to the shape of the form factor as we have mentioned above. But while the one pion system is tapering off, it seems the two pion system has only just begun increasing. Going to even higher values of b_W should then bring the contribution from the two different pion systems closer together, meaning the system would be primarily dominated by the contribution from the pions.

5.2.3 Range parameters at different coupling strengths

While the coupling strength has a minimal effect on the contribution of the second pion, the range parameter has quite a significant effect. So far, all the variations of the range parameter has been at a constant of $S_W = 20MeV$. Let us investigate the effect of changing the coupling strength to other values and varying b_W. We have chosen two different values for the coupling strength, $S_W = 5MeV$ and $S_W = 80MeV$. We vary the coupling range at each of these coupling strengths in order to gauge the contribution of the second pion more accurately.

When the coupling is low, we saw in fig. 5.3 that the contributions from the first and the second pion were closer together. As such, we should expect the contributions from the one pion system and the two pion system to remain a lot closer at all values of b_W. Additionally, the increase in influence of wither of the two systems should happen at later values of b_W, due to their lower coupling. So while the one pion contribution will still be the more dominating of the two different pion contributions, we expect the two pion contribution to play a larger role compared to when we set $S_W = 20MeV$. Alternatively, when $S_W = 80MeV$, the pion contributions should reside entirely with the one pion system, and increases in b_W should have less of an effect on the contribution from the second pion.

We begin by considering the case of $S_W = 5MeV$ in fig. 5.11.

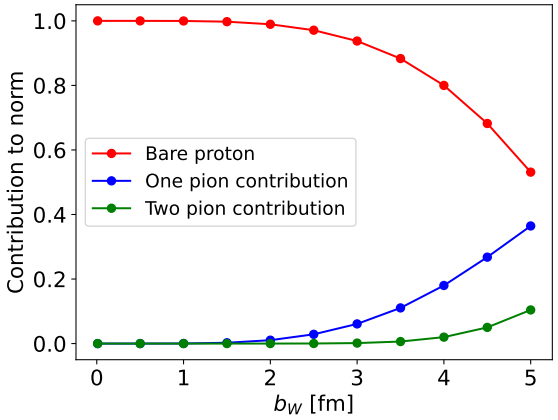

FIGURE 5.10: The contribution to the norm of the wavefunction for the different systems as a function of b_W. The coupling strength has been set to a value of $S_W = 5MeV$. Since the coupling strength is lower, the general contribution from the pion systems is a lot lower. More notably, it appears the two pion system and one pion system are a lot closer to each other.

As fig. 5.10 shows, the one pion and two pion contribution are now a lot closer at most values, only starting to deviate considerably when $b_W = 2.5$. Moreover, we see a significantly larger contribution from the two pion system, which can be seen in fig. 5.11.

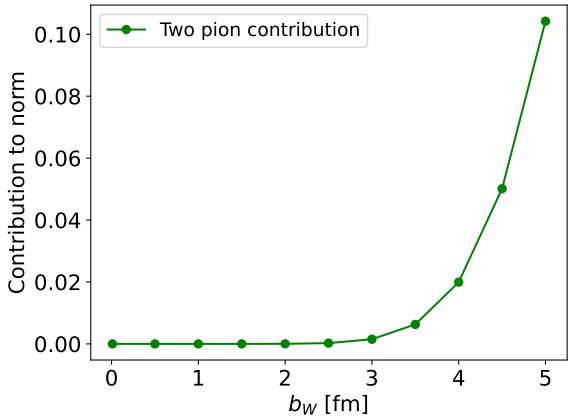

FIGURE 5.11: The contribution to the norm of the wavefunction from the second pion as a function of b_W. The coupling strength has been set to a value of $S_W = 5MeV$. Since the one pion system now has a lower contribution, the two pion system can be seen to have a higher contribution to the norm.

While the increase in contribution happens a bit later compared to when $S_W = 20MeV$ in fig. 5.7, it grows a lot faster, reaching contributions over 10% of the total norm for the values of b_W considered. This makes good sense since the one pion system is now much weaker coupled, meaning that the two pion system can get a much bigger contribution compared to the one pion system.

Finally, let us consider the case where the coupling strength is large. We set $S_W = 80MeV$ and vary the coupling range, see fig. 5.12.

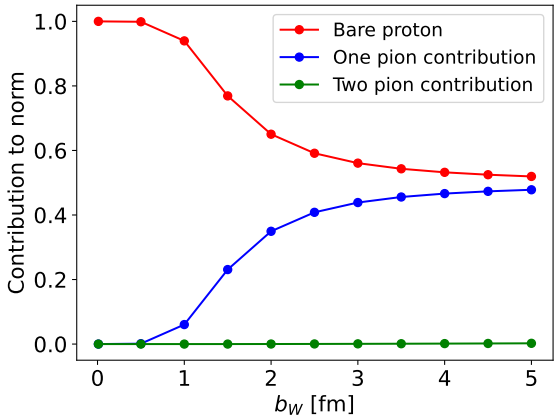

FIGURE 5.12: Contribution to the norm of the wavefunction of the different systems as a function of b_W. The coupling strength has been set to a value of $S_W = 80MeV$. The large coupling strength now completely drowns out the two pion system, and the one pion system dominates completely along with the bare nucleon system.

The system is now entirely dominated by the one-pion contribution and the bare proton contribution. This is as we predicted, based on what we found in fig. 5.4. The contribution from the second pion now remains flat at all values of b_W, and it play no significant part in the contribution to the total overlap.

5.3 Discussion

In fig. 5.1 we have shown that the Gaussian method can solve the system with a single pion with only two Gaussians needed for full convergence toward the final wavefunction. This extends further to the two pion system, as it is clear from fig. 5.2 that the two-pion system converges just as fast. As fig. 5.2 also shows, it is sufficient to use just a single Gaussian in the two-pion system, if the dressed nucleon mass has been found in the one-pion system. One should bear in mind that if other optimization routines, such as the stochastic variational method described in section 2.2, are used then the amount of Gaussians required to reach convergence might increase. This is as of yet unclear.

In fig. 5.3 we showed the contributions of the different systems to the total overlap as a function of coupling strength. Initial observations showed that the contribution from the two pion overlap were significantly smaller than the contribution from the one pion system and the bare nucleon. The contribution from the one pion system grew considerably with increasing coupling strength, eventually becoming similar in size to the contribution of the bare proton, which had the largest contribution of all the systems. A closer investigation in fig. 5.4 and fig. 5.5 showed that the contribution of the second pion peaks when $S_W = 20MeV$, where its contribution was about 0.3%.

Afterwards, the contribution would drop off again. This was a bit surprising, since the parameters of the coupling operator between the bare proton and the one pion system is identical to the parameters between the one pion system and the two pion system. One would therefore expect the contribution of the two pion system to also grow when the coupling strength is increased. A possible explanation for why this is not so, is the fact that the first pion is more strongly bound to the nucleon than the second pion. Then if we increase the coupling strength, the one pion system completely ends up dominating, and the two pion system starts to become much more insignificant. In general though, the two pion contribution is quite weak at all values of S_W, indicating the coupling strength has little influence on the contribution of the second pion.

Whereas we so far haven't seen any significant use of the second pion, this changes with the variation of the range parameter, b_W. This can already be seen in fig. 5.6. The major contributions still come from the one-pion system and the bare nucleon, but we can now see a slight increase in the two pion contribution when b_W reaches 4-5 fm. Looking more closely at fig. 5.7 and fig. 5.8, we see that the contribution from the second pion, along with the energy difference between the two pion system and the one pion system, shows increased contribution to the norm with increasing b_W. It is also apparent from fig. 5.7 that the second pion would contribute more if b_W was increased further. This was explained by the e^{-r^2/b_W} term in eq. (3.9), but since pions are responsible for the long range part of the interaction, one can also use this as an argument for the increase in contribution from the second pion. To investigate this further, we considered more extreme values of b_W, in the range of $5 - 10\,fm$. We saw a notable increase in the contribution from the second pion, along with the contribution from the bare nucleon falling below the contribution of the first pion. Crucially, we could also notice how the effects of the first pion began to taper off, meaning the second pion contribution increased relative to the contribution of the first pion.

As an extra measure, we changed the coupling strength to two values, one lower than $S_W = 20MeV$ and one higher, and redid the variation of the coupling range. The results for the lower coupling strength showed an increase in the contribution from the two pion system, since the one pion system was now more weakly coupled. This makes good sense, since we saw in fig. 5.3 that the one and two pion systems were closest when the coupling strength was low. On the other hand, when the coupling strength was high, variations in b_W made no significant impact on the two pion contribution, even when b_W was set to around $5\,fm$. This also makes sense, since we saw the influence of the second pion drop off at large values of S_W, whereas the one pion system increased in influence. It is then clear, that the one pion approximation is best in cases where the coupling strength is high, but can also work at lower coupling strengths if b_W is sufficiently low.

Chapter 6

Conclusion

In this thesis we have investigated the dressing of the nucleon by a second pion in a nuclear model with explicit pions. We introduced the model in chapter 3, where we derived the general shape of the wavefunctions. We wrote the wavefunctions as a linear combination of correlated Gaussians, which we introduced as a concept in chapter 2. Using this Gaussian expansion, we could find the ground state energy of our system by optimizing a generalized eigenvalue problem, employing both linear and non-linear optimization methods. The necessary matrix elements needed to solve the system of a nucleon dressed with two pions was derived in chapter 4. We developed a general expansion method of the matrix elements, that was usable for any of the matrix elements that were required to solve the system. This general expansion method involved writing out the full pion matrix elements in terms of the spin space identity, and then considering the different components. This method holds for any number of pions and for any matrix element we have considered, however the process becomes quite lengthy already with the addition of a second pion.

Initial solutions to the one-pion system showed the system converging to the expected ground state energy after just 1-2 Gaussians, making it a very capable and efficient method for solving the system. We then considered the addition of the second pion, and investigated its influence as a function of the coupling parameters. We showed that an increase in the coupling strength between the systems has a minimal impact on the contribution of the second pion, with the contribution initially increasing with increased coupling strength but then eventually falling off again. The one pion contribution could be seen to increase when the coupling strength was increased. However, when the coupling range was varied, the contribution from the second pion increased, which suggests that the effects of the second pion cannot be neglected when the range parameter is increased. Varying the coupling range at different coupling strengths, we found that the contribution of the second pion is greatest when the coupling strength is low, and the range parameter is high.

Appendix A

Derivation of Analytical Matrix Elements of Shifted Gaussians

The matrix elements needed to solve eq. (2.11) can be solved analytically and then used to calculate numerical results. In this section, we present the analytical form of the overlap, kinetic energy and coulomb matrix elements. The approach for calculating the form of the matrix elements follows the approach found in [10].

A.1 Overlap

The overlap between to Gaussians with parameter matrices A and B can be calculated by performing the integral of the product of the two shifted Gaussians with respect to all the spatial coordinates that are being considered,

$$\langle G'|G\rangle = \int d^3\vec{r}_1 \dots d^3\vec{r}_N e^{-\mathbf{r}^T C\mathbf{r}+(s+s')^T\mathbf{r}} \tag{A.1}$$

where $C = A + B$. The exponential of the Gaussians can be rewritten in terms of sums.

$$\int d^3\vec{r}_1 \dots d^3\vec{r}_N e^{-\mathbf{r}^T C\mathbf{r}+(s+s')^T\mathbf{r}} = \int d^3\vec{r}_1 \dots d^3\vec{r}_N exp\left(-\sum_{i,j}^{N} C_{i,j}\vec{r}_i\cdot\vec{r}_j + \sum_{i}^{N}(\vec{s}_i + \vec{s'}_i)\cdot\vec{r}_i\right) \tag{A.2}$$

Now, we can exploit that A and B are symmetric matrices, which means that C is also a symmetric matrix. This means we can perform a unitary transform of the coordinates and paramter matrices. Let $\mathbf{r} = Q\mathbf{x}$, where $\mathbf{x}$ is a new set of spatial coordinates and Q is a unitary matrix. Since C is symmetric, there exists a Q such that $C = Q^T DQ$, where D is a diagonal matrix. This means we can rewrite eq. (A.2) into a form where we only integrate over the dot product of similar spatial coordinates.

$$\langle G'|G\rangle = \int d^3\vec{x}_1 \dots d^3\vec{x}_N exp\left(-\sum_i^N D_{i,i}\vec{x}_i^2 + \sum_i^N (\vec{s}_i + \vec{s'}_i)\cdot\vec{x}_i\right) \tag{A.3}$$

Now, using the properties of the exponential function, we can write out the integral in eq. (A.3) as a product of integrals.

$$\begin{aligned}&\int d^3\vec{x}_1 \dots d^3\vec{x}_N exp\left(-\sum_i^N D_{i,i}\vec{x}_i^2 + \sum_i^N (\vec{s}_i + \vec{s'}_i)\cdot\vec{x}_i\right) = \\ &\prod_{i=1}^N \int d^3\vec{x}_i exp\left(-D_{i,i}\vec{x}_i^2 + (\vec{s}_i + \vec{s'}_i)\cdot\vec{x}_i\right)\end{aligned} \tag{A.4}$$

Solving this integral and then transforming back, we end up with the final result

$$\langle G'|G\rangle = \prod_{i=1}^N exp\left(\frac{1}{4D_{i,i}(\vec{s}_i + \vec{s'}_i)^2}\right)\left(\frac{\pi^N}{D_{i,i}}\right)^{3/2} = e^{\frac{1}{4}(s+s')^T R(s+s')}\left(\frac{\pi^N}{det(C)}\right)^{3/2} = M \tag{A.5}$$

where $R = C^{-1}$.

A.2 Kinetic Energy

The general kinetic energy operator is written in matrix notation as.

$$\hat{K} = -\frac{\partial}{\partial \mathbf{r}^T} K \frac{\partial}{\partial \mathbf{r}} \tag{A.6}$$

where K is a symmetric and positive definite matrix. Thus, we want to calculate the following quantity:

$$\langle G'| - \frac{\partial}{\partial \mathbf{r}^T} K \frac{\partial}{\partial \mathbf{r}} |G\rangle \tag{A.7}$$

In order to calculate the overlap of $\hat{K}$, we first prove two sub-results. First, we can consider the overlap with $\mathbf{r}$ by taking the derivative of the shift vectors, $v = s + s'$ in eq. (A.5).

$$\langle G'|\mathbf{r}|G\rangle = \frac{\partial}{\partial v}\left(e^{\frac{1}{4}v^T R v}\left(\frac{\pi^N}{det(C)}\right)^{3/2}\right) = -\frac{1}{2} RvM \tag{A.8}$$

The second sub-result we will need is the following:

$$\langle G'|\mathbf{r}^T F\mathbf{r}|G\rangle = \left(\frac{\partial}{\partial v^T}F\frac{\partial}{\partial v}\right)e^{\frac{1}{4}v^T Rv}\left(\frac{\pi^N}{det(C)}\right)^{3/2} = \left(\frac{3}{2}Trace(FR) - \frac{1}{4}v^T RFRv\right)M \tag{A.9}$$

We can now calculate the derivative in eq. (A.7), and then use eq. (A.8) and eq. (A.9) to get the general result for the kinetic matrix element.

$$\begin{aligned}\langle G'|-\frac{\partial}{\partial \mathbf{r}^T}K\frac{\partial}{\partial \mathbf{r}}|G\rangle &= \langle G'|\left(s'-2A\mathbf{r}\right)^T K\left(s-2B\mathbf{r}\right)|G\rangle \\ &= \left(6Trace(AKBR)\left(s'-AR(s+s')\right)^T K\left(s-BR(s+s')\right)\right)\end{aligned} \tag{A.10}$$

with

$$G' = e^{-\mathbf{r}^T A\mathbf{r}+s'^T\mathbf{r}}, \quad G = e^{-\mathbf{r}^T B\mathbf{r}+s^T\mathbf{r}} \tag{A.11}$$

A.3 Potential Energy Functions

Lastly, we want to consider the overlap of Gaussians with some potential energy function, $V(w^T\mathbf{r})$, where w is a size-N vector with $w_i = 1$ and $w_j = -1$. That is, the quantity $w^T\mathbf{r}$ gives us the difference between the coordinates of the i'th and the j'th particle. We can determine an expression for the overlap of some general potential, $V(w^T\mathbf{r})$ by considering the Fourier transform, $\mathcal{V}(\vec{k})$, of such a potential.

$$\langle G'|V(w^T\mathbf{r})|G\rangle = \int\frac{d^3\vec{k}}{(2\pi)^3}\mathcal{V}(\vec{k})\langle G'|e^{i\vec{k}\cdot(w^T\mathbf{r})}|G\rangle \tag{A.12}$$

The overlap with the exponential function can easily be solved using the methods from eq. (A.3). The end result is an integral of the form

$$\langle G'|V(w^T\mathbf{r})|G\rangle = M\int\frac{d^3\vec{k}}{(2\pi)^3}\mathcal{V}(\vec{k})e^{-\frac{1}{4}w^T Rwk^2+i\vec{k}\cdot q}, \tag{A.13}$$

where M is the expression found in eq. (A.5). Replacing the Fourier transformed function in eq. (A.13) with its untransformed counterpart gives an integral equation over the $\vec{r}$ component.

$$\langle G'|V(w^T\mathbf{r})|G\rangle = M\left(\frac{\beta}{\pi}\right)^{3/2}\int d^3\vec{r}V(\vec{r})e^{-\beta(\vec{r}-q)^2} \tag{A.14}$$

where $\beta = \left(w^T Rw\right)^{-1}$ and $q = \frac{1}{2}w^T R(s+s')$. Of particular interest is the $1/r$ potential associated with the Coulomb force between charged particles. This force is only dependent on the inverse radial distance between the two particles. To calculate

this, we first rewrite eq. (A.14) for the case where $V(\vec{r})$ only depends on the radial distance between two particles. As such, we can carry out the angular derivatives in eq. (A.14), leaving just the integral over the radial components.

$$\langle G'|V(|w^T\mathbf{r}|)|G\rangle = M\left(\frac{\beta}{\pi}\right)^{3/2} 2\pi\frac{e^{-\beta q^2}}{\beta q}\int_0^\infty drrV(r)e^{-\beta r^2}sinh\left(2\beta qr\right) \tag{A.15}$$

Plugging in the $1/r$ potential in equation eq. (A.15) then yields

$$\langle G'|\frac{1}{|w^T\mathbf{r}|}|G\rangle = M\frac{erf\left(\sqrt{\beta}q\right)}{q} \tag{A.16}$$

where $erf()$ is the error function.

Appendix B

Preliminary Calculations using Correlated Gaussians

In order to investigate the functionality of the matrix elements we found in section 4.1, we use them to describe and simulate simple quantum mechanical systems. Even though these matrix elements have been derived with the purpose of calculating the pion matrix elements, they are completely general, and can be modified to suit many few-body systems after need. These simulations serve as a proof of concept for the method, and were used to find errors and bugs in the matrix elements before moving to more complicated systems.

In this chapter, we consider the simulation of the ground state, and the first two excited states of the hydrogen atom using correlated Gaussians.

B.1 The Hydrogen Atom

The hydrogen atom consists of a heavy proton and a single electron orbiting around the proton, bound by the coulomb attraction between the two. Due to the proton being much heavier than the electron, the proton can be considered stationary. This is an extremely simple system, making it adequate for testing the matrix elements we have derived in section 4.1.

We look to solve the following Schrödinger equation, written in units of Hartree and Bohr radius [22]:

$$-\frac{1}{2}(u'' + \left(\frac{2}{r} - \frac{l(l+1)}{r^2}\right) u) = Eu \tag{B.1}$$

where u is the wavefunction we wish to solve, and r is the radial distance. This differential equation can be solved analytically using a Power Series, which yields the radial equations.

$$R_{nl} = \frac{1}{r}\left(\frac{r}{n}\right)^{l+1} e^{-\frac{r}{n}} v\left(\frac{r}{n}\right) \tag{B.2}$$

where $v\left(\frac{r}{n}\right)$ is polynomial of degree $n-l-1$.

$$v\left(\frac{r}{n}\right) = \sum_{j=0}^{n-l-1} c_j \left(\frac{r}{n}\right)^j \tag{B.3}$$

where n is the principal quantum number and l is the quantum number that is associated with the quantized angular momentum. When comparing the wavefunctions, we vary both the principle quantum number, n along with the angular momentum quantum number, l. In short, we shall consider the three radial wavefunctions

$$R_{10} = 2e^{-r} \tag{B.4}$$

$$R_{21} = \frac{1}{2\sqrt{6}} r e^{-r/2} \tag{B.5}$$

$$R_{32} = \frac{4}{81\sqrt{30}} r^2 e^{-r/3} \tag{B.6}$$

The energy levels have a well-known form. When written in units of Hartree, the energy levels become

$$E = \frac{-0.5}{n^2} \tag{B.7}$$

such that the ground state energy is exactly -0.5.

Now, we can express our wavefunctions in a Gaussian basis. This must be done such that the wavefunctions are eigenfunctions of the $\hat{\mathbf{L}}^2$ operator. Writing out the operator in its full form using spherical coordinates, we get [23].

$$\hat{\mathbf{L}}^2 = -\left(\frac{1}{sin(\theta)}\frac{\partial}{\partial\theta}(sin(\theta)\frac{\partial}{\partial\theta}) + \frac{1}{sin^2(\theta)}\frac{\partial^2}{\partial^2\phi}\right) \tag{B.8}$$

and for an eigenfunction of the angular momentum squared, we must have

$$\hat{\mathbf{L}}^2\psi_{nlm} = l(l+1)\psi_{nlm} \tag{B.9}$$

Using eq. (B.8), we can determine how to represent eqs. (B.4) to (B.6) using Gaussians. This leads us to the following expressions.

$$G_{10} = e^{-\alpha r^2} \tag{B.10}$$

$$G_{21} = x e^{-\alpha r^2} \tag{B.11}$$

$$G_{32} = xy e^{-\alpha r^2} \tag{B.12}$$

where x and y are cartesian coordinates, such that $r = \sqrt{x^2+y^2+z^2}$. It can be shown by applying eq. (B.8) to eqs. (B.10) to (B.12) that these are indeed eigenfunctions

of the total angular momentum squared. As such, these are valid candidates for Gaussian representations of our three radial wavefunctions. Solving the generalized eigenvalue problem, using the general expansion in section 4.1, we get the energy convergence graphs in figs. B.1 to B.3. We see from figs. B.1 to B.3 that we converge towards the final energy after roughly 4-5 Gaussians.

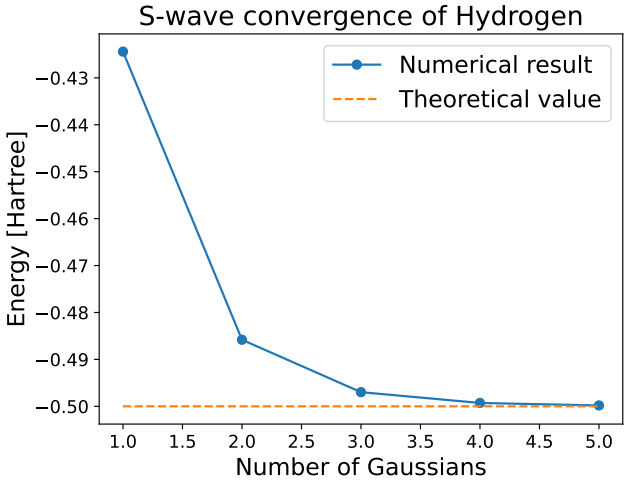

FIGURE B.1: Convergence towards the Hydrogen ground state energy as a function of Gaussians.

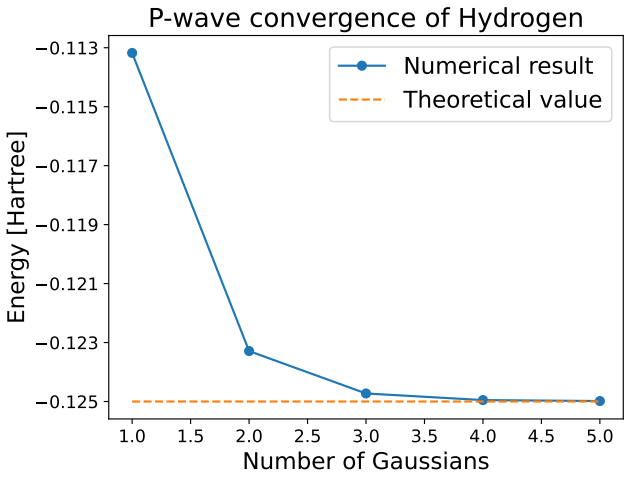

FIGURE B.2: Convergence towards the first excited state of hydrogen as a function of Gaussians.

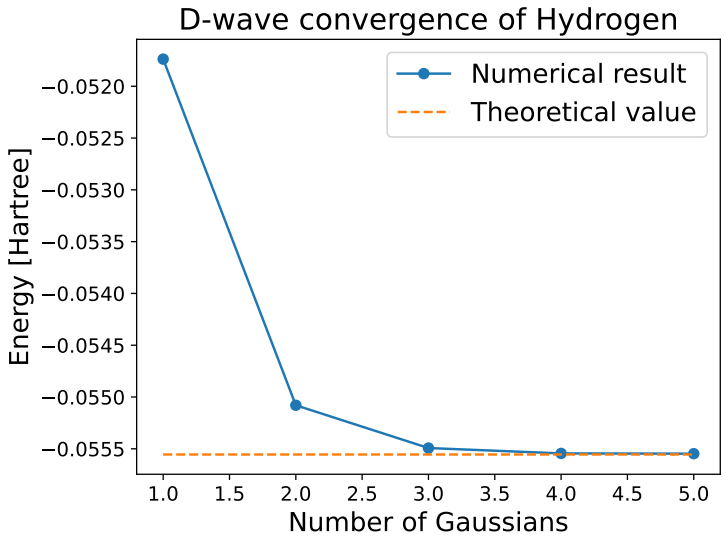

FIGURE B.3: Convergence towards the second excited state of hydrogen as a function of Gaussians.

At 5 Gaussians, the deviation from the accepted values is roughly 0.02%, which is way within reason for most intents and purposes. One should note that the convergence rate varies from problem to problem. Therefore, it is not guarenteed that we can obtain the same level of precision with just five Gaussians, if applied to another problem.

As well as plotting the energy, we can plot the relevant wavefunctions for each of the three states. This can be seen in figs. B.4 to B.6.

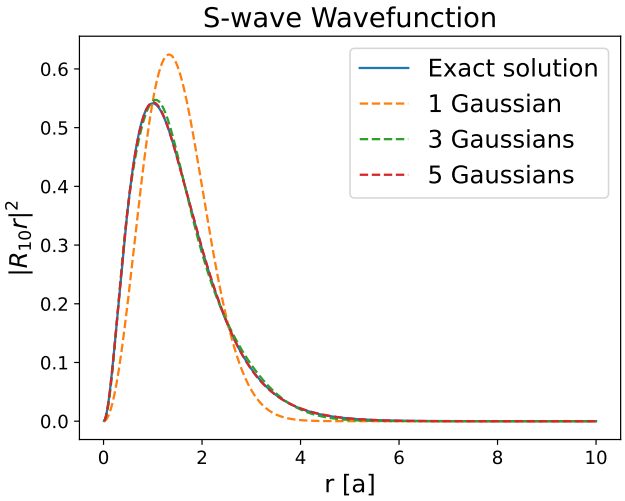

FIGURE B.4: Radial wavefunction of the R_{10} state of hydrogen atom plotted with Gaussians and compared to the actual result.

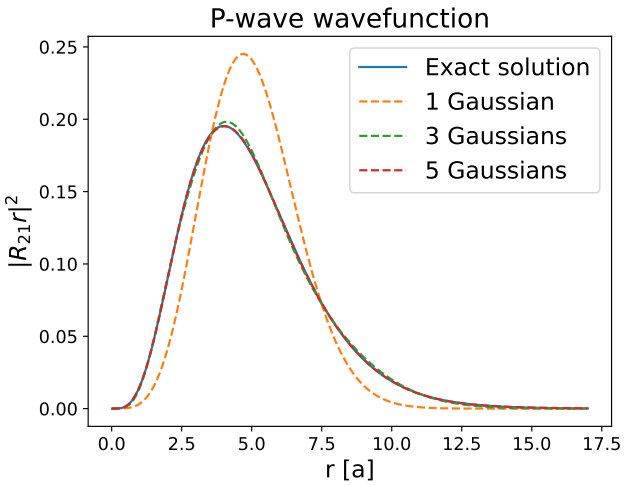

FIGURE B.5: Radial wavefunction of the R_{21} state of hydrogen atom plotted with Gaussians and compared to the actual result.

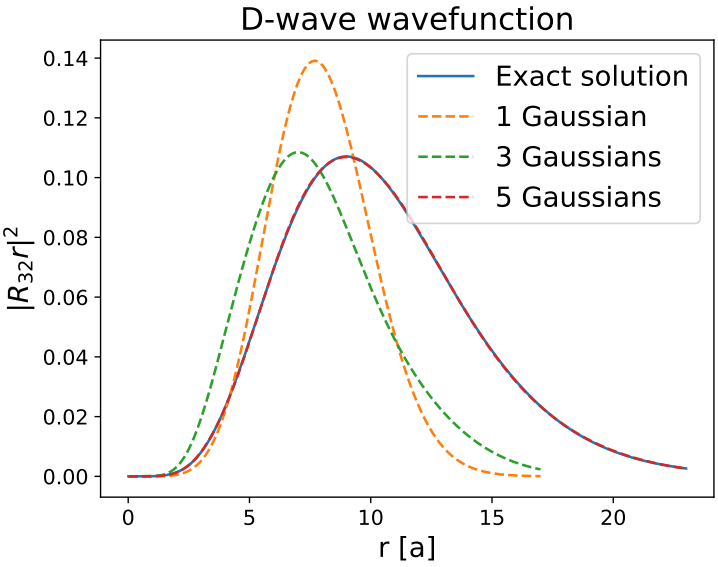

FIGURE B.6: Radial wavefunction of the R_{10} state of hydrogen atom plotted with Gaussians and compared to the actual result.

As with the energy graphs, figs. B.1 to B.3, we see that 1 Gaussian is insufficient to accurately describe the hydrogen atom. For S and P waves, 3 Gaussians do a decent job of accurately following the exact solution, but for D-waves, 3 Gaussians is not enugh to describe the system accurately. 5 Gaussians gives an almost exact solution to the states of the Hydrogen atom. This proves that the general expansion of the

matrix elements have been performed correctly, and that they can be applied to other systems.

Appendix C

Expansion of the kinetic matrix elements

This appendix demonstrates the P- and D-wave expansions of the kinetic matrix element, which we presented in section 4.1. The overlap of the kinetic operator with shifted Gaussians is

$$\langle G^A|\hat{K}|G'^B\rangle = \Big(6Trace(AKBR) + \big(s - RA(s+s')\big)^T K \big(s' - BR(s+s')\big)\Big) M$$

For both the P- and the D-wave expansions, it is beneficial to consider the derivative elements termwise. For the P-wave expansion, carrying out the derivatives term by term we get.

Term 1:

$$\left(\mathbf{a}^T \frac{\partial}{\partial s^T}\right)\left(\mathbf{b}^T \frac{\partial}{\partial s'^T}\right) 6Trace(AKBR)M \xrightarrow{s,s'\to 0} 6Trace(AKBR)M_1 \tag{C.1}$$

Term 2:

$$\left(\mathbf{a}^T \frac{\partial}{\partial s^T}\right)\left(\mathbf{b}^T \frac{\partial}{\partial s'^T}\right) s^T K s' M \xrightarrow{s,s'\to 0} \mathbf{a}^T K \mathbf{b} M_0 \tag{C.2}$$

Term 3:

$$\left(\mathbf{a}^T \frac{\partial}{\partial s^T}\right)\left(\mathbf{b}^T \frac{\partial}{\partial s'^T}\right) - s^T KBR(s+s')M \xrightarrow{s,s'\to 0} -\mathbf{a}^T KBR\mathbf{b} M_0 \tag{C.3}$$

Term 4:

$$\left(\mathbf{a}^T \frac{\partial}{\partial s^T}\right)\left(\mathbf{b}^T \frac{\partial}{\partial s'^T}\right) - (s+s')^T ARK s' M \xrightarrow{s,s'\to 0} -\mathbf{a}^T ARK\mathbf{b} M_0 \tag{C.4}$$

Term 5:

$$\begin{aligned}&\left(\mathbf{a}^T \frac{\partial}{\partial s^T}\right)\left(\mathbf{b}^T \frac{\partial}{\partial s'^T}\right) (s+s')^T RAKBR(s+s')M \\ &\xrightarrow{s,s'\to 0} \mathbf{a}^T ARKBR\mathbf{b} + \mathbf{b}^T ARKBR\mathbf{a} M_0\end{aligned} \tag{C.5}$$

Similarly, the D-wave expansion of the matrix elements can be split term wise as follows.

Term 1:

$$\left(\mathbf{a}^T\frac{\partial}{\partial s^T}\right)\left(\mathbf{b}^T\frac{\partial}{\partial s^T}\right)\left(\mathbf{c}^T\frac{\partial}{\partial s'^T}\right)\left(\mathbf{d}^T\frac{\partial}{\partial s'^T}\right)6Trace(AKBR)M \xrightarrow{s,s'\to 0} 6Trace(AKBR)M_2 \tag{C.6}$$

Term 2:

$$\left(\mathbf{a}^T\frac{\partial}{\partial s^T}\right)\left(\mathbf{b}^T\frac{\partial}{\partial s^T}\right)\left(\mathbf{c}^T\frac{\partial}{\partial s'^T}\right)\left(\mathbf{d}^T\frac{\partial}{\partial s'^T}\right)s^TKs'M \xrightarrow{s,s'\to 0} \frac{1}{2}\left[\left(\mathbf{a}^TK\mathbf{c}\right)\left(\mathbf{b}^TR\mathbf{d}\right)+\left(\mathbf{a}^TK\mathbf{d}\right)\left(\mathbf{b}^TR\mathbf{c}\right)\right]M_0 + \frac{1}{2}\left[\left(\mathbf{b}^TK\mathbf{c}\right)\left(\mathbf{a}^TR\mathbf{d}\right)+\left(\mathbf{b}^TK\mathbf{d}\right)\left(\mathbf{a}^TR\mathbf{c}\right)\right]M_0 \tag{C.7}$$

Term 3:

$$\left(\mathbf{a}^T\frac{\partial}{\partial s^T}\right)\left(\mathbf{b}^T\frac{\partial}{\partial s^T}\right)\left(\mathbf{c}^T\frac{\partial}{\partial s'^T}\right)\left(\mathbf{d}^T\frac{\partial}{\partial s'^T}\right)-s^TKBR(s+s')M \xrightarrow{s,s'\to 0} -\frac{1}{2}\left[\left(\mathbf{c}^TKBR\mathbf{a}\right)\left(\mathbf{b}^TR\mathbf{d}\right)+\left(\mathbf{c}^TKBR\mathbf{b}\right)\left(\mathbf{a}^TR\mathbf{d}\right)+\left(\mathbf{c}^TKBR\mathbf{d}\right)\left(\mathbf{a}^TR\mathbf{b}\right)\right]M_0 - \frac{1}{2}\left[\left(\mathbf{d}^TKBR\mathbf{a}\right)\left(\mathbf{b}^TR\mathbf{c}\right)+\left(\mathbf{d}^TKBR\mathbf{b}\right)\left(\mathbf{a}^TR\mathbf{c}\right)+\left(\mathbf{d}^TKBR\mathbf{c}\right)\left(\mathbf{a}^TR\mathbf{b}\right)\right]M_0 \tag{C.8}$$

Term 4:

$$\left(\mathbf{a}^T\frac{\partial}{\partial s^T}\right)\left(\mathbf{b}^T\frac{\partial}{\partial s^T}\right)\left(\mathbf{c}^T\frac{\partial}{\partial s'^T}\right)\left(\mathbf{d}^T\frac{\partial}{\partial s'^T}\right)-(s+s')^TRAKs'M \xrightarrow{s,s'\to 0} -\frac{1}{2}\left[\left(\mathbf{a}^TRAK\mathbf{b}\right)\left(\mathbf{c}^TR\mathbf{d}\right)+\left(\mathbf{b}^TRAK\mathbf{a}\right)\left(\mathbf{c}^TR\mathbf{d}\right)\right]M_0 - \frac{1}{2}\left[\left(\mathbf{c}^TRAK\mathbf{a}\right)\left(\mathbf{b}^TR\mathbf{d}\right)+\left(\mathbf{c}^TRAK\mathbf{b}\right)\left(\mathbf{b}^TR\mathbf{d}\right)\right]M_0 - \frac{1}{2}\left[\left(\mathbf{d}^TRAK\mathbf{a}\right)\left(\mathbf{b}^TR\mathbf{c}\right)+\left(\mathbf{d}^TRAK\mathbf{b}\right)\left(\mathbf{a}^TR\mathbf{c}\right)\right]M_0 \tag{C.9}$$

Term 5:

$$\left(\mathbf{a}^T\frac{\partial}{\partial s^T}\right)\left(\mathbf{b}^T\frac{\partial}{\partial s^T}\right)\left(\mathbf{c}^T\frac{\partial}{\partial s'^T}\right)\left(\mathbf{d}^T\frac{\partial}{\partial s'^T}\right)(s+s')^TRAKBR(s+s')M \xrightarrow{s,s'\to 0} \frac{1}{2}\left[\left(\mathbf{a}^TRAKBR\mathbf{b}\right)\left(\mathbf{c}^TR\mathbf{d}\right)+\left(\mathbf{a}^TRAKBR\mathbf{c}\right)\left(\mathbf{b}^TR\mathbf{d}\right)+\left(\mathbf{a}^TRAKBR\mathbf{d}\right)\left(\mathbf{c}^TR\mathbf{d}\right)\right]M_0 + \frac{1}{2}\left[\left(\mathbf{b}^TRAKBR\mathbf{a}\right)\left(\mathbf{c}^TR\mathbf{d}\right)+\left(\mathbf{b}^TRAKBR\mathbf{c}\right)\left(\mathbf{a}^TR\mathbf{d}\right)+\left(\mathbf{b}^TRAKBR\mathbf{d}\right)\left(\mathbf{a}^TR\mathbf{c}\right)\right]M_0 + \frac{1}{2}\left[\left(\mathbf{c}^TRAKBR\mathbf{a}\right)\left(\mathbf{b}^TR\mathbf{d}\right)+\left(\mathbf{c}^TRAKBR\mathbf{b}\right)\left(\mathbf{a}^TR\mathbf{d}\right)+\left(\mathbf{c}^TRAKBR\mathbf{d}\right)\left(\mathbf{a}^TR\mathbf{b}\right)\right]M_0 + \frac{1}{2}\left[\left(\mathbf{d}^TRAKBR\mathbf{a}\right)\left(\mathbf{b}^TR\mathbf{c}\right)+\left(\mathbf{d}^TRAKBR\mathbf{b}\right)\left(\mathbf{a}^TR\mathbf{c}\right)+\left(\mathbf{d}^TRAKBR\mathbf{c}\right)\left(\mathbf{a}^TR\mathbf{b}\right)\right]M_0 \tag{C.10}$$

Appendix D

Coulomb Interactions in the Nuclear Model with Explicit Pions

In chapter 3 and chapter 4 we have argued that the exclusion of Coulomb interactions is a small correction. In this chapter, we show explicitly why Coulomb interactions can be omitted.

First, let us explicitly consider the isospin structure of the proton. The proton exists in a coherent superposition of several pions. The one pion system has no coulomb interactions when applied to the proton, so we consider only the two pion system.

$$\begin{aligned}&\left(\vec{\tau}\cdot\vec{\pi}_1\right)\left(\vec{\tau}\cdot\vec{\pi}_2\right)p=\\&p\pi_1^0\pi_2^0+\sqrt{2}n\pi_1^+\pi_2^0-\sqrt{2}n\pi_1^0\pi_2^++4p\pi_1^-\pi_2^+\end{aligned}\tag{D.1}$$

The only term where Coulombic interactions are relevant is the last term. As such, when constructing the matrix matrix elements of the Hamiltonian, the kinetic terms are multiplied by a factor of 9, and the Coulombic terms are multiplied by 4. If we write the radial component of the Gaussian wavefunction as $\psi_{\tilde{N}\pi\pi}(r)$, we can write the two-pion component as

$$\langle\psi^A_{\tilde{N}\pi\pi}|\hat{K}+V_C|\psi^B_{\tilde{N}\pi\pi}\rangle=9\langle\psi^A_{\tilde{N}\pi\pi}(r)|\hat{K}|\psi^B_{\tilde{N}\pi\pi}(r)\rangle+4\langle\psi^A_{\tilde{N}\pi\pi}(r)|V_C|\psi^B_{\tilde{N}\pi\pi}(r)\rangle\tag{D.2}$$

	Energy	contribution to overlap
With Coulomb	-587.5621	0.0018868
Without Coulomb	-587.5618	0.0018861

Table D.1: Caption.

The effect of the Coulombic interactions can be seen in table D.1. The parameters used are the same parameters used when showing the initial energy convergence plot, fig. 5.2 in section 5.1. We have set $S_W = 41.5MeV$ and $b_W = 3.9fm$. The table shows an energy difference in the energy at the third decimal place while, while the contribution to the overlap is different at the seventh decimal place. These differences are so small that they can easily be neglected.

Bibliography

[1] R. Machleidt. "Historical perspective and future prospects for nuclear interactions". In: *International Journal of Modern Physics E* 26.11 (2017), p. 1730005. DOI: 10.1142/S0218301317300053. URL: https://doi.org/10.1142/S0218301317300053.

[2] Hideki Yukawa. "On the Interaction of Elementary Particles. I". In: *Proceedings of the Physico-Mathematical Society of Japan. 3rd Series* 17 (1935), pp. 48–57. DOI: 10.11429/ppmsj1919.17.0_48.

[3] Gerald A. Miller. "The Fundamental Nature of Low-Energy Pion-Nucleon Interactions". In: (2022). DOI: https://doi.org/10.48550/arXiv.2208.12873. URL: https://arxiv.org/abs/2208.12873.

[4] Ronald A. Bryan and Bruce L. Scott. "Nucleon-Nucleon Scattering from One-Boson-Exchange Potentials". In: *Phys. Rev.* 135 (2B July 1964), B434–B450. DOI: 10.1103/PhysRev.135.B434. URL: https://link.aps.org/doi/10.1103/PhysRev.135.B434.

[5] Steven Weinberg. "Nuclear forces from chiral lagrangians". In: *Physics Letters B* 251.2 (1990), pp. 288–292. DOI: https://doi.org/10.1016/0370-2693(90)90938-3. URL: https://www.sciencedirect.com/science/article/pii/0370269390909383.

[6] D. V. Fedorov. "A Nuclear Model with Explicit Mesons". In: *Few-Body Systems* 61.4 (2020). DOI: 10.1007/s00601-020-01573-1. URL: https://doi.org/10.1007%2Fs00601-020-01573-1.

[7] D. V. Fedorov and M. Mikkelsen. "Threshold Photoproduction of Neutral Pions Off Protons in Nuclear Model with Explicit Mesons". In: *Few-Body Systems* 64.1 (2022). DOI: 10.1007/s00601-022-01783-9. URL: https://doi.org/10.1007%2Fs00601-022-01783-9.

[8] Jim Mitroy et al. "Theory and application of explicitly correlated Gaussians". In: *Rev. Mod. Phys.* 85 (2 May 2013), pp. 693–749. DOI: 10.1103/RevModPhys.85.693. URL: https://link.aps.org/doi/10.1103/RevModPhys.85.693.

[9] Emiko Hiyama. "Gaussian expansion method for few-body systems and its applications to atomic and nuclear physics". In: *Progress of Theoretical and Experimental Physics* 2012.1 (Sept. 2012). 01A204. DOI: 10.1093/ptep/pts015. URL: https://doi.org/10.1093/ptep/pts015.

[10] D. V. Fedorov. “Analytic Matrix Elements and Gradients with Shifted Correlated Gaussians”. In: *Few-Body Systems* 58.1 (Dec. 2016). DOI: 10.1007/s00601-016-1183-0. URL: https://doi.org/10.1007%2Fs00601-016-1183-0.

[11] D. V. Fedorov. “Correlated Gaussians and Low-Discrepancy Sequences”. In: *Few-Body Systems* 60.3 (2019). DOI: 10.1007/s00601-019-1521-0. URL: https://doi.org/10.1007%2Fs00601-019-1521-0.

[12] Jun J. Sakurai and Jim Napolitano. *Modern quantum mechanics*. eng. 2nd ed. Cambridge: Cambridge University Press, 2017.

[13] Beresford N. Parlett. *The Symmetric Eigenvalue Problem*. eng. Englewood Cliffs: Prentice-Hall, 1980.

[14] *Documentation page for scipy.linalg.eigh*. URL: https://docs.scipy.org/doc/scipy/reference/generated/scipy.linalg.eigh.html (visited on 06/06/2023).

[15] Pauli Virtanen et al. “SciPy 1.0: fundamental algorithms for scientific computing in Python”. In: *Nature Methods* 17.3 (Feb. 2020), pp. 261–272. DOI: 10.1038/s41592-019-0686-2. URL: https://doi.org/10.1038%2Fs41592-019-0686-2.

[16] Yasuyuki Suzuki and Kálmán Varga. *Stochastic Variational Approach to Quantum-Mechanical Few-Body Problems*. eng. Vol. 54. Lecture Notes in Physics Monographs. Berlin, Heidelberg: Springer Berlin / Heidelberg, 1998.

[17] J. A. Nelder and R. Mead. “A Simplex Method for Function Minimization”. In: *The Computer Journal* 7.4 (Jan. 1965), pp. 308–313. DOI: 10.1093/comjnl/7.4.308. URL: https://doi.org/10.1093/comjnl/7.4.308.

[18] Phillip J. Siemens and Aksel S. Jensen. *Elements of nuclei : many-body physics with the strong interaction*. eng. Lecture notes and supplements in physics. Redwood City, Calif: Addison-Wesley, 1987.

[19] László Jenkovszky, István Szanyi, and Chung-I Tan. “Shape of proton and the pion cloud”. In: *The European Physical Journal A* 54.7 (July 2018). DOI: 10.1140/epja/i2018-12567-5. URL: https://doi.org/10.1140%2Fepja%2Fi2018-12567-5.

[20] Martin Mikkelsen. “Threshold Pion Photoproduction off Nucleons using the Nuclear Model with Explicit Pions”. Master’s thesis in physics, Aarhus University. Nov. 2022.

[21] A. Zee. *Group theory in a nutshell for physicists*. eng. In a nutshell. Princeton, New Jersey: Princeton University Press, 2016.

[22] D. R. Hartree. “The Wave Mechanics of an Atom with a Non-Coulomb Central Field. Part I. Theory and Methods”. In: *Mathematical Proceedings of the Cambridge Philosophical Society* 24.1 (1928), pp. 89–110. DOI: 10.1017/S0305004100011919.

[23] David J. Griffiths. *Introduction to quantum mechanics*. eng. Third edition. Cambridge, United Kingdom: Cambridge University Press, 2018.